

**Preparation and Characterization of Well-defined Fe/SiO₂ Spherical Catalysts for
Fischer Tropsch Synthesis (FTS)**

By

FAISAL BIN MOHAMAD YUSOFF

Dissertation submitted in partial fulfillment of

The requirements for the

Bachelor of Engineering (Hons)

(Chemical Engineering)

JUNE 2009

Universiti Teknologi Petronas

Bandar Seri Iskandar

31750 Tronoh

Perak Darul Ridzuan

CERTIFICATION OF APPROVAL

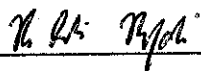
**Preparation and Characterization of Well-defined Fe/SiO₂ Spherical Catalysts for
Fischer Tropsch Synthesis (FTS)**

by

Faisal bin Mohamad Yusoff

A project dissertation submitted to the
Chemical Engineering Programme
Universiti Teknologi PETRONAS
in partial fulfillment of the requirement for the
BACHELOR OF ENGINEERING (Hons)
(CHEMICAL ENGINEERING)

Approved by,



(A.P Dr. Noor Asmawati M. Zabidi)

UNIVERSITI TEKNOLOGI PETRONAS

TRONOH, PERAK

JUNE 2009

CERTIFICATION OF ORIGINALITY

This is to certify that I am responsible for the work submitted in this project, that the original work is my own except as specified in the references and acknowledgements, and that the original work contained herein have not been undertaken or done by unspecified sources or persons.



FAISAL B. MOHAMAD YUSOFF

ABSTRACT

The aim of this project is to study the preparation methods of iron nanocatalysts on SiO₂ support for the Fischer Tropsch synthesis (FTS). The first phase is to prepare and characterize the silica spheres. In the second phase, iron nanocatalysts were synthesized and deposited on the silica support. Iron particles were synthesized using the ammonia deposition method and impregnation method. The iron metal was attached to silica spheres which have BET surface area of 61m²/g at 2, 3 and 5wt% loadings. Variables such as the metal loading, ageing time and calcinations temperatures were studied during the catalysts preparation. There are two methodologies that involved in this project which are Ammonia Deposition Method and Impregnation Method. Different loadings will result a different color of the sample and different results for characterization. There are several ways of characterization that will involved in this project such as Scanning Electron Microscope (SEM), Xray Diffraction (XRD), Transmission Electron Microscope (TEM), Energy Dispersive Xray (EDX) . EDX analysis showed the presence of Si, O and Fe elements in the catalyst. The TEM images from 5wt% impregnated catalyst showed iron particles with diameter ranging from 19 nm to 34 nm deposited on silica spheres. The average diameter of SiO₂ sphere is 168nm. The inconsistencies of metal attachments on the silica for impregnation method seem to be due to inefficient stirring during preparation. XRD analysis indicates the amorphous nature of the catalyst.

ACKNOWLEDGEMENT

First and foremost I would like to praise Allah S.W.T The Most Gracious, The Most Merciful for blessing me from day one.

My deepest appreciation goes to my supervisor, A.P Dr. Noor Asmawati M.Zabidi. She has supervised, guided and gave out precious comments and ideas in completing this project throughout the semester. Her encouragements and willingness to provide constructive critics and suggestions are much appreciated.

My deepest gratitude goes to Mr. Jailani and Mr. Yusof from the Laboratory Department who has given me the light and guided me in an area in which I am very unfamiliar with. Words cannot express how much I appreciate their time and efforts in helping me accomplish a large part of this project.

I would also like to express a special thanks to Mr. M. Tazli Azizan, the Final Year Research Project (FYRP) Coordinator for his efforts in making sure that all resources are made available so that the students can conduct their FYRP successfully.

And most important of all, to my family for their undying love and motivation in seeing I successfully pull off another great chapter in my life's journal as a student. I would not have made it through these period of this FYRP without their strength and support. Last but not least to all my fellow course mates for sharing all the tough moments that sometimes can be daunting, in completing this Final Year Research project.

TABLE OF CONTENTS

CERTIFICATIONS	<i>i</i>
ABSTRACT	<i>iii</i>
ACKNOWLEDGEMENT	<i>iv</i>
CHAPTER 1- INTRODUCTION	<i>1</i>
1.1 Problem Statement.....	<i>1</i>
1.2 Objectives & Scope Study.....	<i>1</i>
CHAPTER 2-LITERATURE REVIEW	<i>3</i>
2.1 Fischer-Tropsch Catalyst.....	<i>3</i>
2.2 Fischer-Tropsch Process.....	<i>4</i>
2.3 Process Condition.....	<i>5</i>
2.4 Silica Particles.....	<i>6</i>
2.5 Characterization of Catalysts.....	<i>6</i>
2.6 High-Resolution Transmission Microscope.....	<i>7</i>
2.7 X-Ray Characterization of Nanoparticles.....	<i>9</i>
2.8 Scanning Electron Microscope.....	<i>10</i>
2.9 Physical Aspect of Adsorption.....	<i>13</i>
CHAPTER 3-METHODOLOGY	<i>15</i>
3.1 Research & Experimental Project.....	<i>15</i>
3.2 Chemicals and Quantity.....	<i>16</i>
3.3 Tools and Equipment.....	<i>16</i>

3.4 Preparation of Silica Spheres Support.....	17
3.5 Catalyst Preparation.....	22
CHAPTER 4 – RESULTS AND DISCUSSION	26
4.1 Silica preparation.....	26
4.2 Catalyst preparation (Ammonia Method).....	31
4.3 Catalyst preparation (Impregnation Method).....	36
4.4 Comparison of Impregnation Method & Ammonia Deposition Method	44
CHAPTER 5- CONCLUSION AND RECOMMENDATIONS	45
REFERENCES.....	47

LIST OF FIGURES

Figure 2.1:	The organization of the transmission electron microscope	8
Figure 2.2:	Picture of a Philips transmission electron microscope with the column and viewing screen readily visible	8
Figure 2.3:	The electron optical column and differential pumping system of the environmental scanning electron microscope	11
Figure 3.1:	Mixture start to stir and change to milky white	19
Figure 3.2:	Sample going into rotary evaporator and after that into o	19
Figure 3.3:	Sample going into furnace and then being grind.	21
Figure 3.4:	Preparation of catalyst using Ammonia Deposition method.	23
Figure 3.5:	Preparation of 5wt% Fe/SiO ₂ using impregnation method	25

Figure 4.1:	The isotherm plot on silica spheres	30
Figure 4.2:	Adsorption isotherms	30
Figure 4.3:	Comparing the color of different loading of Fe / SiO ₂ catalyst	32
Figure 4.4:	Scanning Electron Microscope image of 5wt% Fe / SiO ₂ loading	34
Figure 4.5:	The composition graph of 5wt% Fe / SiO ₂ loading	34
Figure 4.6:	Comparing the color of different loading of Fe / SiO ₂ catalyst	37
Figure 4.7:	Scanning Electron Microscope image of 5wt% Fe / SiO ₂ loading	38
Figure 4.8:	The composition graph of 5wt% Fe / SiO ₂ loading	38
Figure 4.9:	Transmission Electron Microscopy (TEM) image of the synthesized silica spheres	40
Figure 4.10	Transmission Electron Microscopy (TEM) image of the synthesized silica spheres	40
Figure 4.11	Transmission Electron Microscopy (TEM) image of 5wt% Fe/SiO ₂ catalyst of impregnation method	41
Figure 4.12	TEM image of 5wt% Fe/SiO ₂ catalyst with different iron size attached on the silica	42
Figure 4.13	XRD result for 3wt% Fe/SiO ₂ catalyst by impregnation	43

LIST OF TABLES

Table 3.1:	List of chemicals and the quantity for the experiment.	16
Table 3.1:	List of equipments that will used during the experimental hours	16
Table 4.1:	Summary of preparing a silica support spheres	28
Table 4.2:	Summary of silica spheres photograph	29
Table 4.3:	Summary of observation of ammonia deposition method	32
Table 4.4:	Summary of metal loading and weight of iron	33

1.0 INTRODUCTION

1.1 Problem Statement

Iron is the transition metals and the fourth most plentiful element in the Earth's crust, is the structural backbone of our modern infrastructure [1]. Iron has been somewhat neglected in favor of its own oxides, as well as other metals such as cobalt, nickel, gold and platinum. Iron's reactivity is important in macroscopic applications but is a dominant concern at the nanoscale. Finely divided iron has long been known to be pyrophoric, which is a major reason that iron nanoparticles have not been more fully studied to date. This extreme reactivity has traditionally made iron nanoparticles difficult to study and inconvenient for practical applications. Iron however has a great deal to offer at the nanoscale, including very potent magnetic and catalytic properties. Iron is a classical catalyst for the Fischer-Tropsch (FT) reaction. It is therefore the size of iron particles affects the product selectivity in FT reaction. In order to perform fundamental study on the catalytic reaction, catalyst model with defined size will be fabricated.

1.2 Objectives and Scope Study

There are several objectives in this project that have been a fundamental of research and laboratory work. There are:

- i. To prepare and characterize a well supported silica spheres.
- ii. To prepare Fe/SiO₂ catalysts using the Ammonia Deposition Method and Impregnation Method.
- iii. To characterize the Fe/SiO₂ catalyst in nanometer size range.

The project involves preparation of the iron nanocatalyst using the ammonia deposition method and impregnation method. The literature of iron nanoparticles as with all nanoparticles is somewhat confused by a lack of consistency in definition and terminology. It has been argued that only particles between 1 and 10nm in size can be regarded as a nanoparticle, based on the SI units system ^[2] or that anything between 1 and 1000nm is a nanoparticle ^[3]. Finely divided iron has been studied for many years, but it has been very difficult until relatively recently to know just what the dimensions of the iron studied were when the particles were smaller than the wavelength of light. Certainly some of the particles studied were nanoparticles, but judging from their methods of preparation, they were likely very polydisperse, and showed great variety in shape. Much of this very early work focused on preparing particles or particle systems and measuring the macroscopic properties of the particles, often magnetic properties such as magnetization and coactivity. Theories were devised to describe the expected magnetic properties of iron nanoparticles, but were difficult to test without an independent measure of the particle sizes and shapes. With the application of electron microscopy to these systems in the 1940s and 1950s, particle sizes, shapes, and distribution information could be readily determined. There was a renewed interest in finely divided iron, as the properties could now be correlated with the sizes and shapes of the particles. By the early 1960s, the theory describing the magnetism of iron nanoparticles was fully formed and had been largely confirmed by experiments. ^[4-8] Research on iron nanoparticles has continued since then, but has experienced a surge in interest in the recent decade or two. This is likely due to new synthetic techniques as well as interest in new applications of iron nanoparticles. In recent years research has continued in earnest, and shows no signs of slowing ^[9].

2.0 LITERATURE REVIEW

2.1 Fischer-Tropsch Catalyst

The production of higher hydrocarbon materials from synthesis gas, i.e. carbon monoxide and hydrogen, commonly known as the Fischer-Tropsch (FT) process, has been in commercial use for many years. Such processes rely on specialized catalysts. The original catalysts for the Fischer-Tropsch synthesis were nickel. Nickel is still the preferred catalyst for hydrogenation of fats and specialty chemicals. Over the years, other metals, particularly iron and cobalt, have been preferred in the Fischer-Tropsch synthesis of higher hydrocarbons whereas copper has been the catalyst of choice for alcohol synthesis. Cobalt is particularly preferred for Fischer-Tropsch synthesis due its high productivity and comparatively low methane selectivity. As the technology of these syntheses developed over the years, the catalysts became more refined and were augmented by other metals and/or metal oxides that function to promote their catalytic activity. These promoter metals include the Group VIII metals, such as platinum, palladium, rhenium, ruthenium and iridium. Metal oxide promoters include the oxides of a broader range of metals, such as molybdenum, tungsten, zirconium, magnesium, manganese and titanium. Those of ordinary skill in the art will appreciate that the choice of a particular metal or alloy for fabricating a catalyst to be utilized in Fischer-Tropsch synthesis will depend in large measure on the desired product or products^[10].

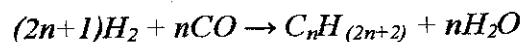
Cobalt catalysts are preferred for Fischer-Tropsch synthesis when the feedstock is natural gas due to the higher activity of the cobalt catalyst. Natural gas has high hydrogen to carbon ratio, so the water-gas-shift is not needed for cobalt catalysts. Iron catalysts are preferred for lower quality feedstocks such as coal or biomass. While iron catalysts are also susceptible to sulfur poisoning from coal with high sulfur content, the lower cost of iron makes sacrificial catalyst at the front of a reactor bed economical. Also, as mentioned earlier, iron can catalyze the water-gas-shift to increase the hydrogen to carbon ratio to make the reaction more favorably selective.

2.2 Fischer-Tropsch Process

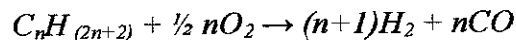
Fischer-Tropsch process is a method for the synthesis of hydrocarbons and other aliphatic compounds^[11]. Synthesis gas, a mixture of hydrogen and carbon monoxide, is reacted in the presence of an iron or cobalt catalyst; much heat is evolved, and such products as methane, synthetic gasoline and waxes, and alcohols are made, with water or carbon dioxide produced as a byproduct. An important source of the hydrogen-carbon monoxide gas mixture is the gasification of coal. The process is named after F. Fischer and H. Tropsch, the German coal researchers who discovered it in 1923.

2.2.1 Original Process of Fischer-Tropsch Synthesis

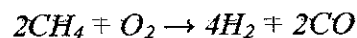
The original Fischer-Tropsch process is described by the following chemical equation (where 'n' is a positive integer)^[12]:



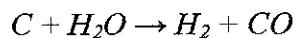
The initial reactants in the above reaction (i.e. CO and H₂) can be produced by other reactions such as the partial combustion of a hydrocarbon:



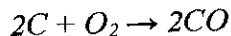
for example (when n=1), methane (in the case of gas to liquids applications):



or by the gasification of coal or biomass:



The energy needed for this endothermic reaction of coal or biomass and steam is usually provided by (exothermic) combustion with air or oxygen. This leads to the following reaction:



The mixture of carbon monoxide and hydrogen is called synthesis gas or syngas. The resulting hydrocarbon products are refined to produce the desired synthetic fuel.

The carbon dioxide and carbon monoxide is generated by partial oxidation of coal and wood-based fuels. The utility of the process is primarily in its role in producing fluid hydrocarbons from a solid feedstock, such as coal or solid carbon-containing wastes of various types. Non-oxidative pyrolysis of the solid material produces syngas which can be used directly as a fuel without being taken through Fischer-Tropsch transformations. If liquid petroleum-like fuel, lubricant, or wax is required, the Fischer-Tropsch process can be applied.

2.3 Process Condition

Generally, the Fischer-Tropsch process is operated in the temperature range of 150-300°C (302-572°F). Higher temperatures lead to faster reactions and higher conversion rates, but also tend to favor methane production. As a result the temperature is usually maintained at the low to middle part of the range. Increasing the pressure leads to higher conversion rates and also favors formation of long-chained alkanes both of which are desirable. Typical pressures are in the range of one to several tens of atmospheres. Chemically, even higher pressures would be favorable, but the benefits may not justify the additional costs of high-pressure equipment.

A variety of synthesis gas compositions can be used. For cobalt-based catalysts the optimal H₂: CO ratio is around 1.8-2.1. Iron-based catalysts promote the water-gas-shift reaction and thus can tolerate significantly lower ratios. This can be important for synthesis gas derived from coal or biomass, which tend to have relatively low H₂: CO ratios.

2.4 Silica Particles

Silica chemistry has been the basis for the catalyst essential in refining crude oil to gasoline and other fuels^[13]. Colloidal silica is used in making the molds for casting the super alloys in jet engines and for polishing silicon wafers in the electronic industry. Pure silica is needed for the glass in fiber optics. The word silica has a very broad connotation. It includes silicon dioxide in all its forms such as crystalline, amorphous, soluble or chemically combined. This includes silicon in any chemically combined form in which the silica atom is surrounded by four or six oxygen atoms. Thus, we can speak of the silica content of clay, or of sodium silicate, in terms of SiO_2 .

2.5 Characterization of Catalysts

Heterogeneous catalysts usually consist of highly divided solid phases that are closely interconnected and thus difficult to characterize. Conventional transmission electron microscopy (CTEM) offers the unique advantages of allowing the direct observation of catalyst morphology with a resolution tunable in the range 10^{-4} - 10^{-10} m and of obtaining structural information by lattice imaging and micro diffraction techniques. Moreover, scanning transmission electron microscope (STEM) equipped with the x-ray analyzers can be used to determine the local composition of catalysts with a spatial resolution as good as 1 nm in the case of field emission gun STEM. This is why electron microscopy is now in widespread use for catalyst characterization.

A few review articles have been devoted to electron microscopy as applied to catalysts characterization, but the recent, rapid development of high resolution analytical microscopy has not been properly covered. The present chapter is intended to give only a brief account of CTEM instrumentation and principles, but application to catalyst morphology and structure characterization will be developed. Emphasis is laid on STEM and its associated analytical capabilities: energy dispersive X-ray emission spectroscopy (EDX), electron energy loss spectroscopy (EELS) and diffraction on

nanodomains (nanodiffraction). More specifically, dedicated STEM, working only in scanning mode, will be considered.

2.6 High-Resolution Transmission Microscope (HRTEM)

The formation of images in the conventional TEM is very similar to that in an optical microscope. The TEM column indicates:

- i. The electron gun, which is either a tungsten filament heated at 2500°C or a LAB₆ cathode heated at 1600°C giving intensity ten times higher. The acceleration voltage is commonly 100-200 kV but higher voltages are available on commercial microscopes.
- ii. The system of condenser lenses gives a demagnified image of the source on the specimen.
- iii. The objective lens gives a magnified image (typically x 100) of the specimen on the image plane.

The specimen should be thin enough (e.g.: less than 100 nm for a 100-kV beam) to transmit the electron beam. The limit of resolution in the absence of lens aberration is $0.61\lambda/\alpha$, where α is the aperture angle of the beam determined by the objective aperture. Lens astigmatism can be corrected by additional coils. The most limiting aberration is spherical, which causes the electron beam to focus in different image planes for different aperture angles α . The aberration is proportional to $C_s \alpha^3$, where C_s is the spherical aberration coefficient and the resolution limit is given by $C_s \alpha^3 + 0.61\lambda/\alpha$.^[16]

This TEM is a microscopy technique whereby a beam of electrons is transmitted through an ultra thin specimen, interacting with the specimen as it passes through it. An image is formed from the electrons transmitted through the specimen, magnified and focused by an objective lens and appears on an imaging screen, a fluorescent screen in most TEMs, plus a monitor, or on a layer of photographic film, or to be detected by a sensor such as a CCD camera.

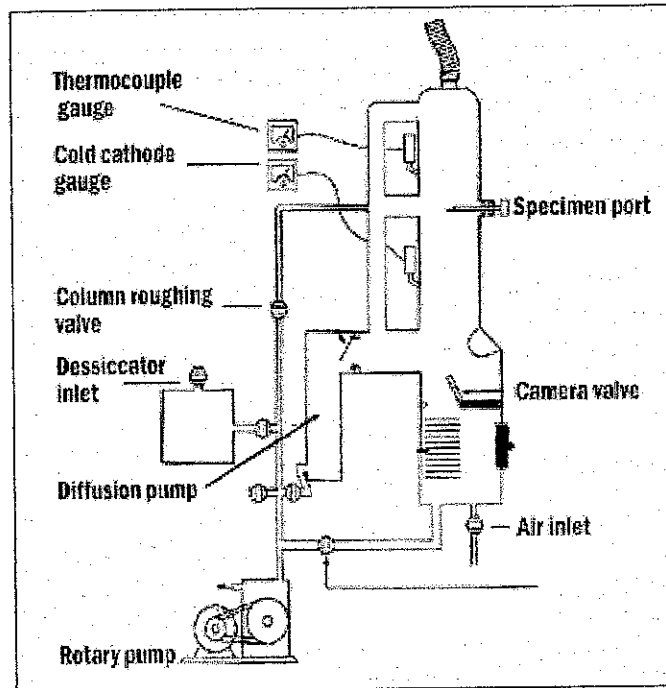


Figure 2.1: *The organization of the transmission electron microscope (TEM)*^[17]

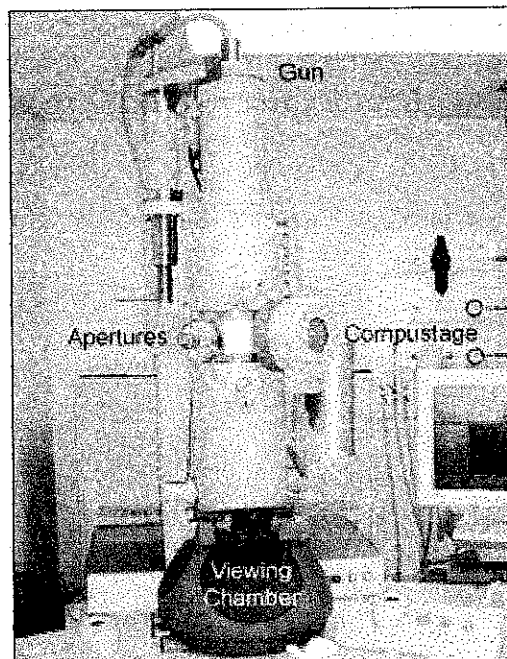


Figure 2.2: *Picture of a Philips transmission electron microscope with the column and viewing screen readily visible*^[17]

2.7 X-Ray Characterization of Nanoparticles

One of the most fundamental characteristics of nanometer-sized particles is their very high surface-to-volume ratio. This can lead to novel and unexpected atomic arrangements, and may also have dramatic effects on the other physical or chemical attributes. Because of this, the precise determination of nanoparticle structure, both medium-range order and/or the existence of local distortion, is a fundamental issue.

It must be recognized that X-Ray diffraction (XRD), based on wide-angle elastic scattering of x-rays, has been the single most important technique for determining the structure of materials characterized by long-range order. However, for other systems, such as disordered materials, XRD has been of limited use, and other experimental techniques have had to be developed. A particularly powerful example is the technique of EXAFS (Extended x-ray absorption fine structure), which probes the local environment of a particular element. Although this method is, as XRD, reciprocal space based, it is essentially a spectroscopic technique, exploiting the energy dependence of x-ray absorption due to interference effects in the individual photoelectron scattering process. The fact allows precise measurement of a local environment without the necessity of long-range order in the material. ^[18]

2.8 Scanning Electron Microscope (SEM)

The scanning electron microscope (SEM) is a type of electron microscope that images the sample surface by scanning it with a high-energy beam of electrons in a raster scan pattern. The electrons interact with the atoms that make up the sample producing signals that contain information about the sample's surface topography, composition and other properties such as The types of signals produced by an SEM include secondary electrons, back scattered electrons (BSE), characteristic x-rays, light (cathodoluminescence), specimen current and transmitted electrons. These types of signal all require specialized detectors for their detection that are not usually all present on a single machine. The signals result from interactions of the electron beam with atoms at or near the surface of the sample. In the most common or standard detection mode, secondary electron imaging or SEI, the SEM can produce very high-resolution images of a sample surface, revealing details about 1 to 5 nm in size. Due to the way these images are created, SEM micrographs have a very large depth of field yielding a characteristic three-dimensional appearance useful for understanding the surface structure of a sample. This is exemplified by the micrograph of pollen shown to the right. A wide range of magnifications is possible, from about x 25 (about equivalent to that of a powerful hand-lens) to about x 250,000, about 250 times the magnification limit of the best light microscopes. Back-scattered electrons (BSE) are beam electrons that are reflected from the sample by elastic scattering. BSE are often used in analytical SEM along with the spectra made from the characteristic x-rays. Because the intensity of the BSE signal is strongly related to the atomic number (Z) of the specimen, BSE images can provide information about the distribution of different elements in the sample. For the same reason BSE imaging can image colloidal gold immuno-labels of 5 or 10 nm diameters, which would otherwise be difficult or impossible to detect in secondary electron images in biological specimens. Characteristic X-rays are emitted when the electron beam removes an inner shell electron from the sample, causing a higher energy electron to fill the shell and release energy. These characteristic x-rays are used to identify the composition and measure the abundance of elements in the sample ^[19].

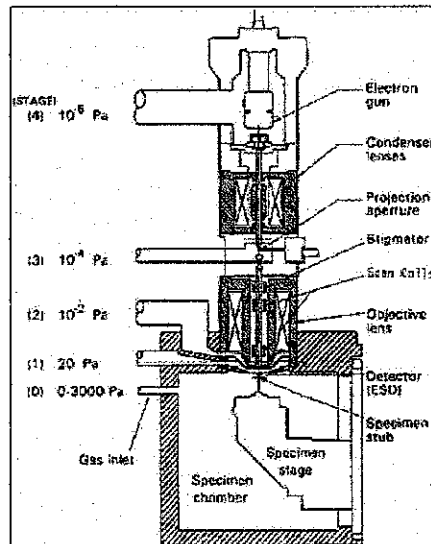


Figure 2.3: *The electron optical column and differential pumping system of the environmental scanning electron microscope*^[17].

In a typical SEM, an electron beam is thermionically emitted from an electron gun fitted with a tungsten filament cathode. Tungsten is normally used in thermionic electron guns because it has the highest melting point and lowest vapour pressure of all metals, thereby allowing it to be heated for electron emission, and because of its low cost. Other types of electron emitters include lanthanum hexaboride (LaB_6) cathodes, which can be used in a standard tungsten filament SEM if the vacuum system is upgraded and field emission guns (FEG), which may be of the cold-cathode type using tungsten single crystal emitters or the thermally-assisted Schottky type, using emitters of zirconium oxide.

The electron beam, which typically has an energy ranging from a few hundred eV to 40 keV, is focused by one or two condenser lenses to a spot about 0.4 nm to 5 nm in diameter. The beam passes through pairs of scanning coils or pairs of deflector plates in the electron column, typically in the final lens, which deflect the beam in the x and y axes so that it scans in a raster fashion over a rectangular area of the sample surface.

When the primary electron beam interacts with the sample, the electrons lose energy by repeated random scattering and absorption within a teardrop-shaped volume of the specimen known as the interaction volume, which extends from less than 100 nm to around 5 μm into the surface. The size of the interaction volume depends on the electron's landing energy, the atomic number of the specimen and the specimen's density. The energy exchange between the electron beam and the sample results in the reflection of high-energy electrons by elastic scattering, emission of secondary electrons by inelastic scattering and the emission of electromagnetic radiation, each of which can be detected by specialized detectors. The beam current absorbed by the specimen can also be detected and used to create images of the distribution of specimen current. Electronic amplifiers of various types are used to amplify the signals which are displayed as variations in brightness on a cathode ray tube. The raster scanning of the CRT display is synchronized with that of the beam on the specimen in the microscope, and the resulting image is therefore a distribution map of the intensity of the signal being emitted from the scanned area of the specimen. The image may be captured by photography from a high resolution cathode ray tube, but in modern machines is digitally captured and displayed on a computer monitor and saved to a computer's hard disc.

2.9 Physical Aspect of Adsorption

2.9.1 Non-porous Solid

The dispersion forces between the adsorptive molecules and surface atoms or ions of the adsorbing solid are described by the Lennard-Jones potential [20].

$$v(r) = -C/r^{-6} + B/r^{-12}$$

Adsorption isotherms can be classified in six types according to IUPAC [21]. The type I is typical for micro porous solids and chemisorptions isotherms. Type II is shown by finely divided nonporous solids. Type III and Type V are typical of vapors. Type IV and Type V feature an hysteresis loop generated by the capillary condensation in mesopores. The rare Type VI, the steps-like isotherm, is shown with nitrogen on special carbons.

Classification of pores according to their width:

- Micropores Less than 2 nm
- Mesopores Between 2 nm and 50 nm
- Macrospores Larger than 50 nm

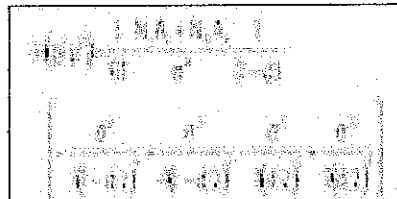
2.9.2 Mesoporous Solid

At low relative pressure of the pore walls adsorbs a multilayer of adsorbate. If the pressure is raised, droplets of adsorbate occur on optimal energetic points of the pore surface with curvatures according to the Kelvin equation. If the droplets touch each other, the pores will be filled with condensed adsorbate. This will evaporate during the desorption from pores showing core openings larger than the Kelvin radius. The adsorption branch is pore-dimension dependant, and the desorption branch is related to the pore openings.

2.9.3 Microporous Solid

In micropores the potentials of both sides of the pore walls overlap, thus enhancing the adsorption potential ^[22]. The smaller the pore width the deeper the resulting potential becomes. This results in enhanced adsorption energy, and adsorption takes place at very low pressure. Micropores with the smaller width fill first, but adsorption on the surface of larger micropores occurs at the same time (secondary micropore filling)

Horvath and Kawazoe ^[23] developed a method to calculate the micropore size distribution according to the relation between the pore width and the resulting adsorption potential. The integration of the potential function gives a relationship between the relative pressure and the pore size:



3.0 METHODOLOGY & PROJECT WORK

3.1 Research & Experimental Project

Basically this project involves preparation of Silica support and preparation of iron nanocatalyst. Early on there several variables that need to be monitor and investigated during the experiment so that the author can have a result that the author need. After doing some research and when doing an ongoing experimental work the author has decided that are two variables that need to take into consideration. The variables that need to be monitor are:

- Metal loading
- Calcinations temperature

The synthesized nonmaterial will be characterized in terms of particles size, porosity, and surface area. The characterization will involve scanning electron microscope (SEM/EDS). It is a type of electron microscope that images the sample surface by scanning it with a high-energy beam of electrons in a raster scan pattern. The electrons interact with the atoms that make up the sample producing signals that contain information about the sample's surface topography, composition and other properties such as electrical conductivity.

3.2 Chemicals and Quantity

No	Chemicals/ Materials	Quantity
1	Fe (NO ₃) ₃ .9H ₂ O	500g
2	Ammonia solution (28wt %)	500g
3	Tetraethyl ortosilicate (TEOS)	500g
4	Ethanol (absolute)	1 Liter

Table 3.1: List of chemicals and the quantity for the experiment.

3.3 Tools and Equipment

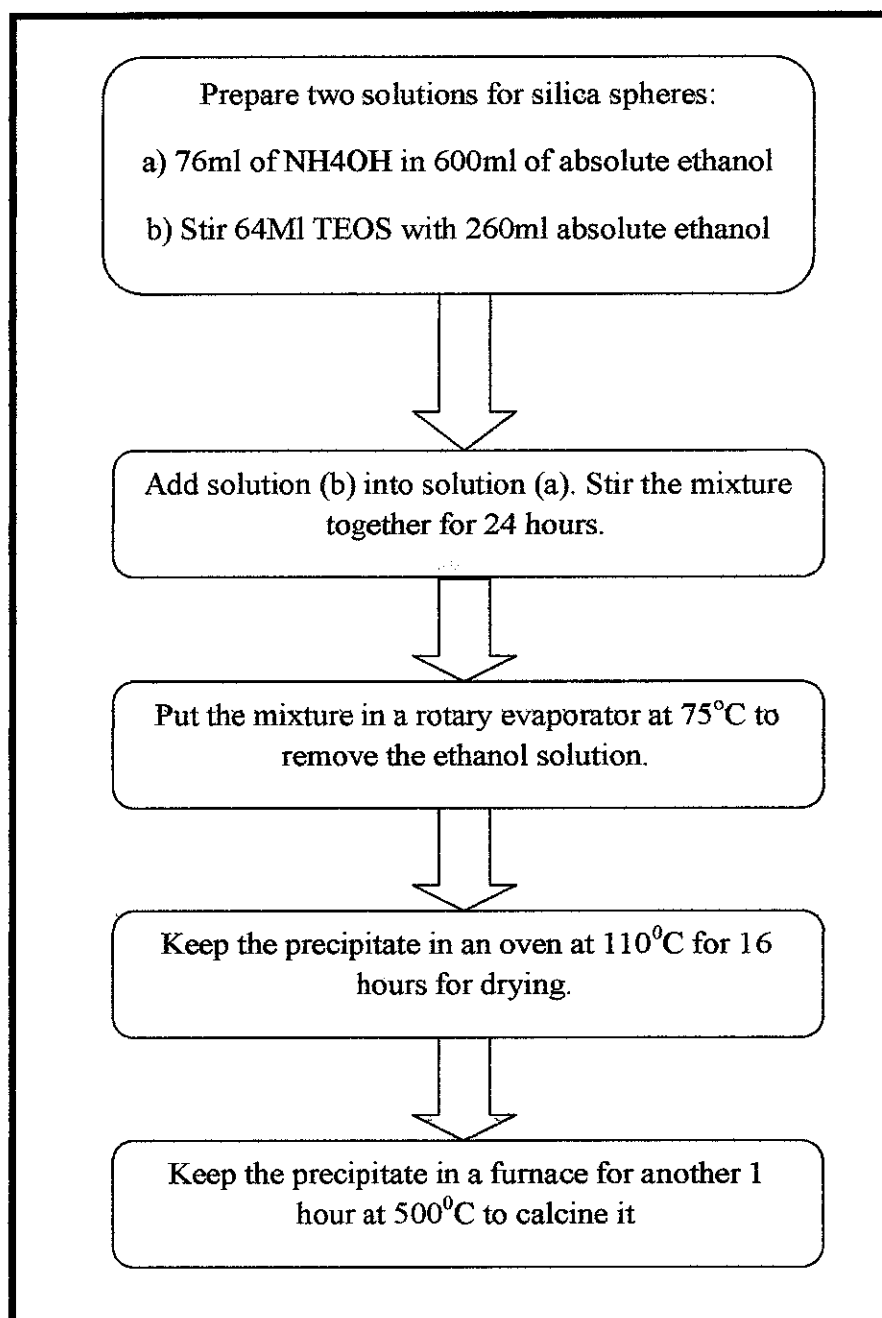
No	Equipment	Quantity
1	Surface area analyzer and temperature-programmed apparatus (TPD/RO)	1
2	BET surface area analyzer	1
3	Transmission electron microscope (TEM)	1
4	Scanning electron microscope	1
5	Rotary evaporator	1
6	Furnace	1
7	Magnetic stirrer/ hot plate	1
8	Conical flask	1

Table 3.2: List of equipments that will used during the experimental hours

3.4 Preparation of Silica Spheres Support

3.4.1 Preparation of nonporous silica spheres

The nonporous silica spheres were prepared as described previously^[24]. Tetraethyl ortosilicate (TEOS) with Merck grade, ethanol (99.9%, Merck grade), distilled water and ammonia (25% Merck grade) were mixed in the prescribed amounts and stirred for 24h in a conical flask^[25]. Then, the silica containing slurry was dried in a rotor evaporator at 75⁰C, to ensure improved handling and maximum recovery of the nonporous silica spheres after the reaction compared with separating the silica spheres by centrifugation. After drying, the silica spheres were calcined at 400⁰C to remove adsorbed ammonia.



Estimated time = 42 hours

3.4.2 Preparation of silica spheres

5th Experiment

Date: **24 February 2009**

Lab: 03-02-05

430pm: chemicals preparation

500pm: start stirring

530pm: colorless mixture start to change into milky white. Stir for 24 hours.

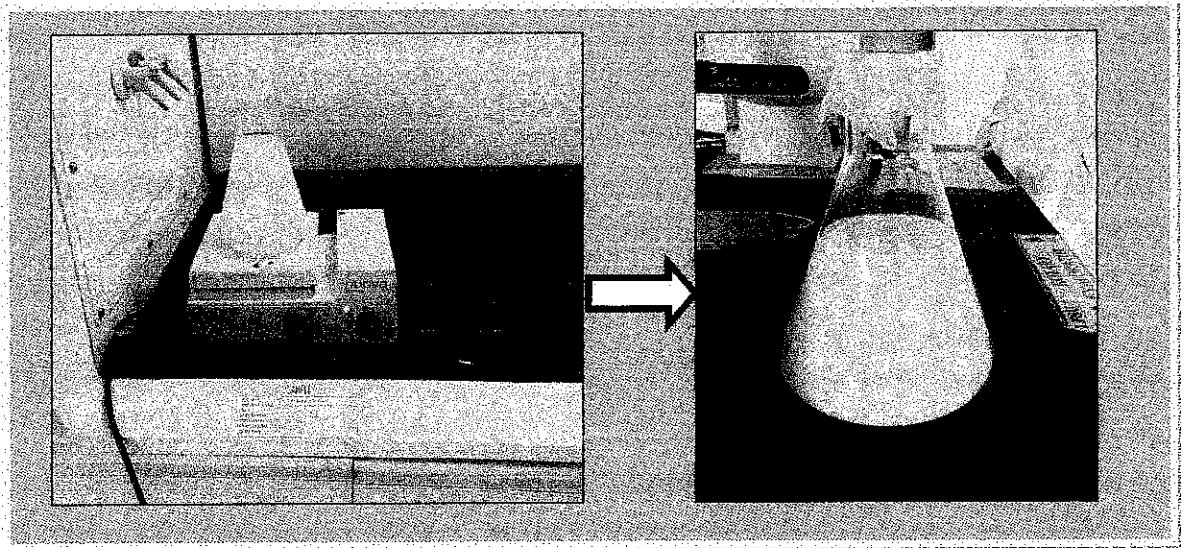


Figure 3.1: *Mixture start to stir and change to milky white*

Date: **25 February 2009**

Lab: 03-02-04

500pm: stop stirring the mixture

505pm: cover up the mixture with parafilm

Date: 26 February 2009

Lab: 03-02-04

1200pm: ethanol start to evaporate (start the rotary evaporator)

[Speed=6; temperature= 75°C]

145pm: stop rotary evaporator

[Notes: weight after = 15.6124g]

500pm: crucible going into furnace for cleaning at 530°C

600pm: sample going into oven for 16hours. Temperature at 110°C.

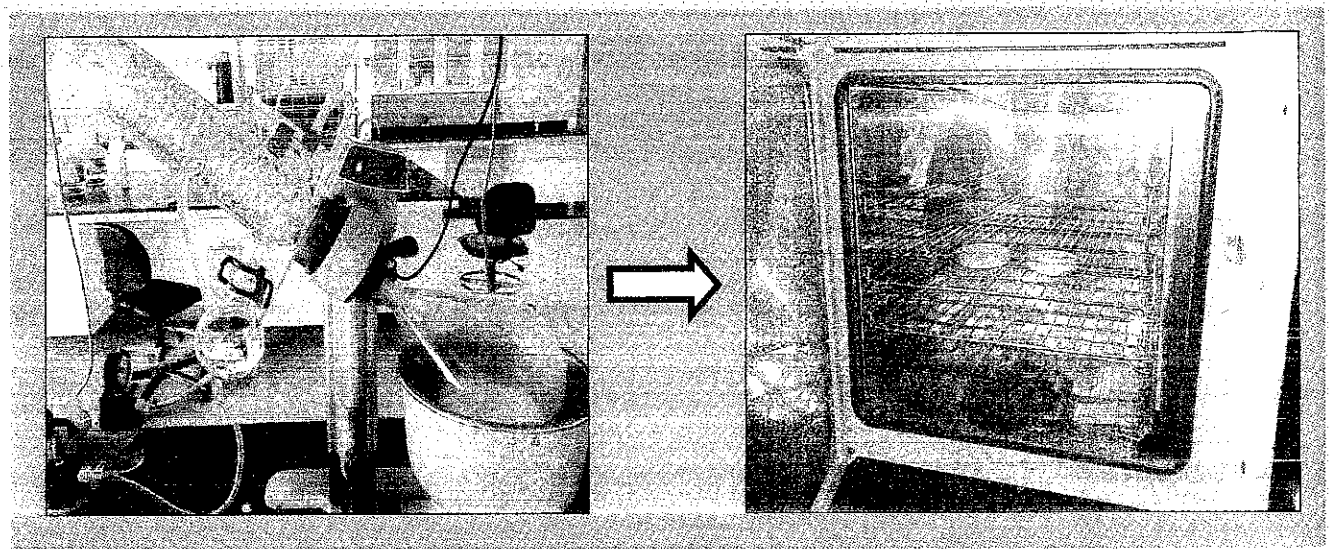


Figure 3.2: Sample going into rotary evaporator and after that into oven

Date: 27 February 2009

Lab: 04-02-17

1000am: Take sample out from the oven. Weight the sample.

[Weight: 14.9976g]

1205pm: Put the sample into furnace at 500°C for an hour.

105pm: Take sample out from the furnace.

[Weight: 14.1373g]

300pm: Start to grind the silica for an hour with mortar and pestel.

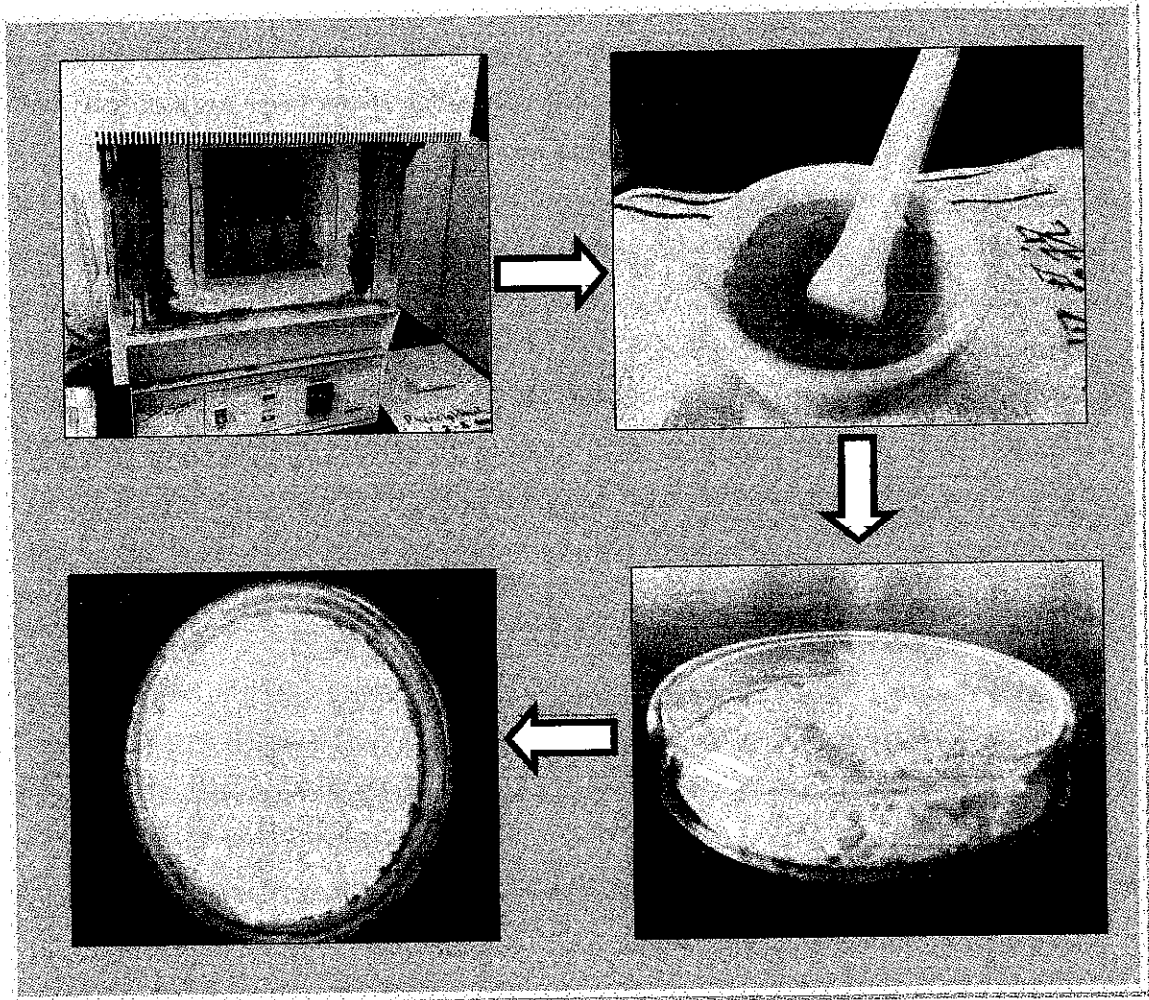
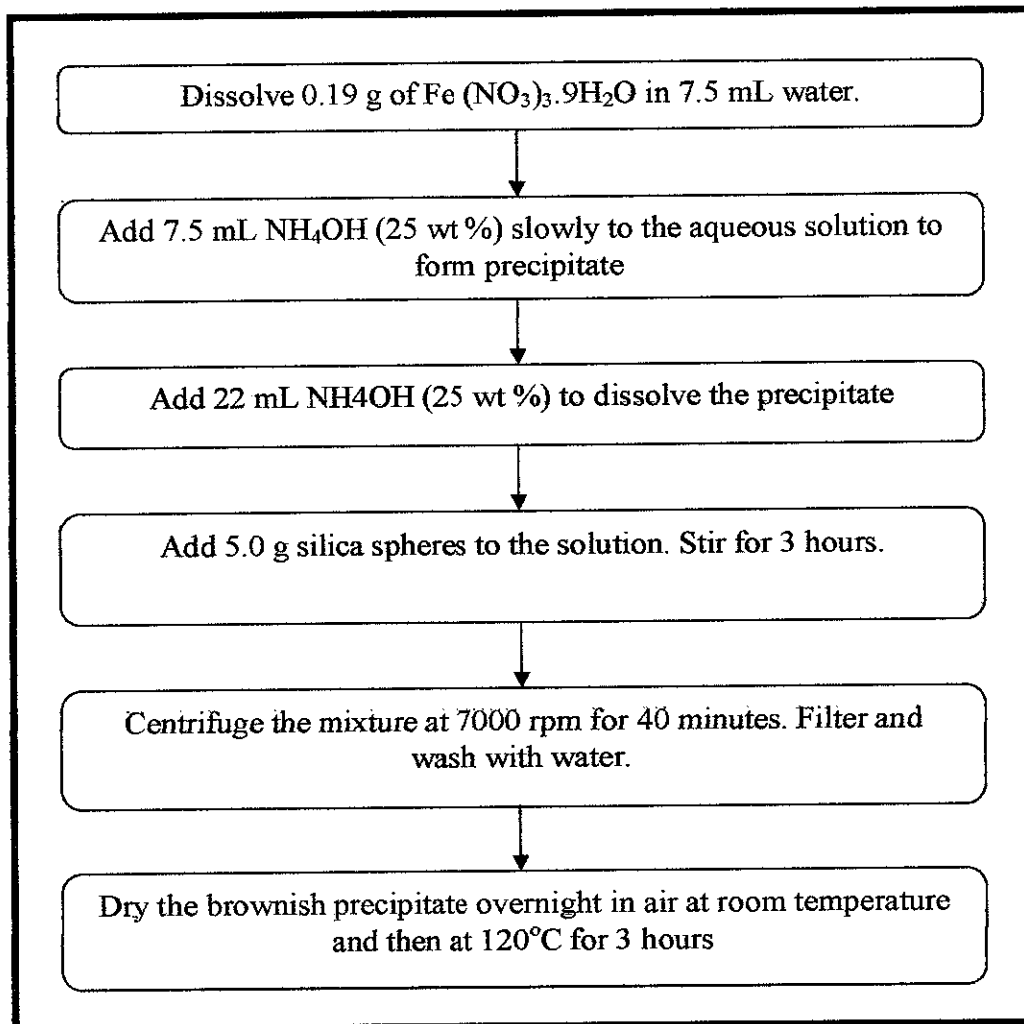


Figure 3.3: *Sample going into furnace and then being grind.*

The sample undergoes BET analysis for characterization.

3.5 Catalyst Preparation

3.5.1 Preparation of 5 wt% spherical Fe/SiO₂ catalysts by ammonia deposition method



The procedures will be repeated at different weight of Fe(NO₃)₃·9H₂O to get different cobalt loading on the catalysts:

- Use 0.11 g Fe(NO₃)₃·9H₂O to get a 3 wt% Fe/SiO₂ catalyst
- Use 0.07 g Fe(NO₃)₃·9H₂O to get a 2 wt% Fe/SiO₂ catalyst

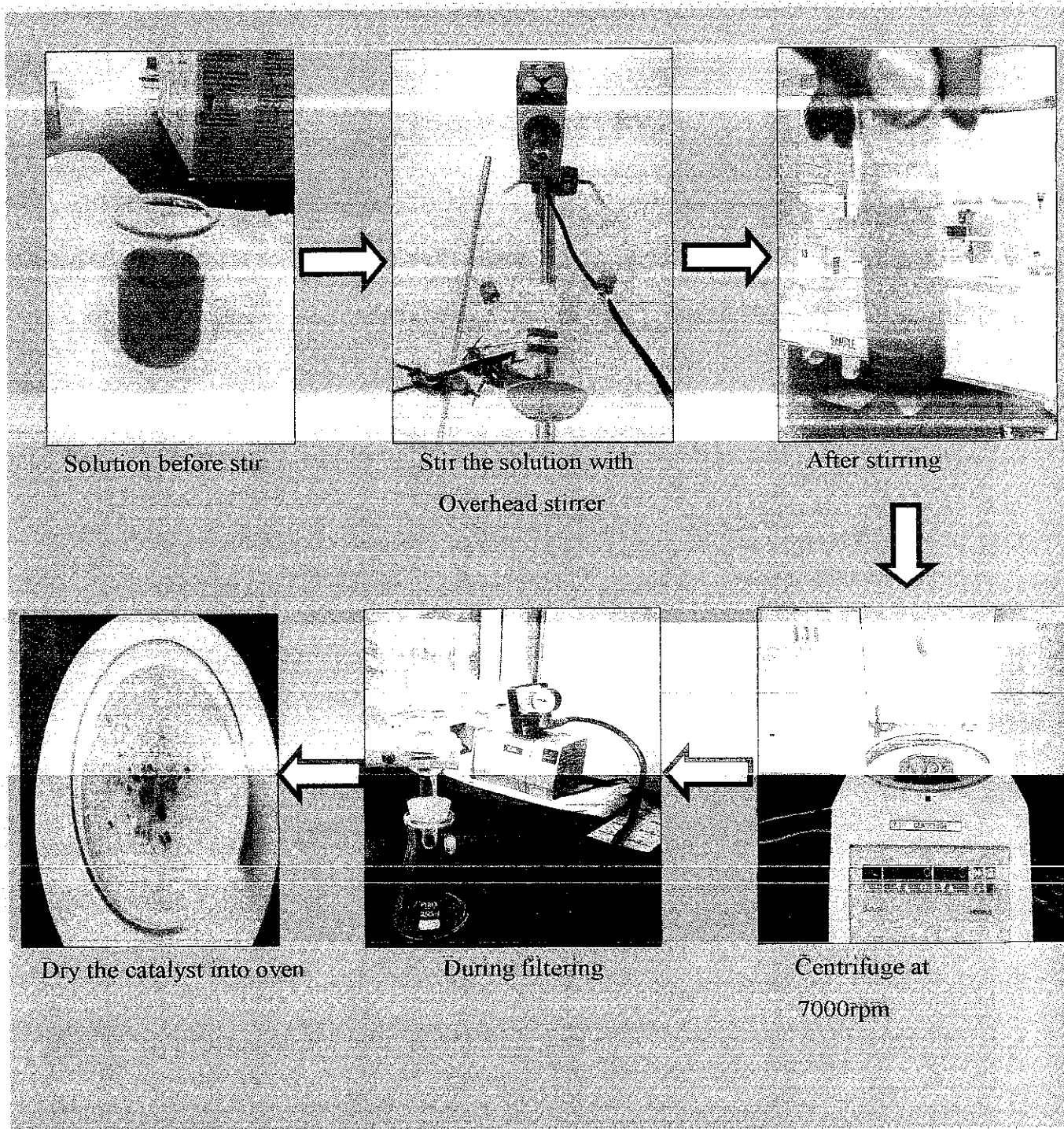
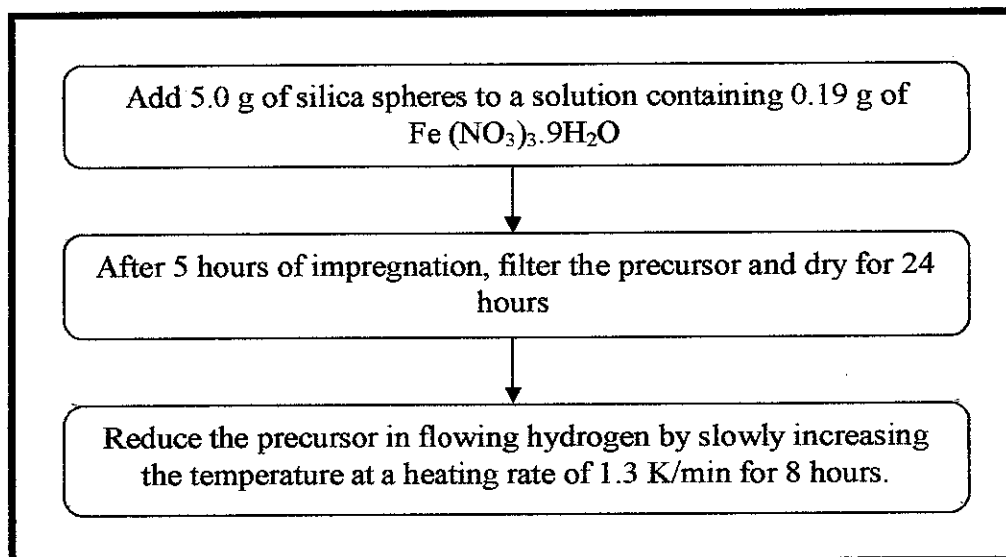


Figure 3.4: Preparation of catalyst using Ammonia Deposition method.

After all this steps, the catalyst is now in the process of characterization by SEM and XRD.

3.5.2 Preparation of 5 wt% spherical Fe/SiO₂ model catalysts by impregnation method



The procedures will be repeated at different weight of Fe (NO₃)₃.9H₂O to get different iron loading on the catalysts:

- i. Use 0.11 g Fe (NO₃)₃.9H₂O to get a 3 wt% Fe/SiO₂ catalyst
- ii. Use 0.07 g Fe (NO₃)₃.9H₂O to get a 2 wt% Fe/SiO₂ catalyst

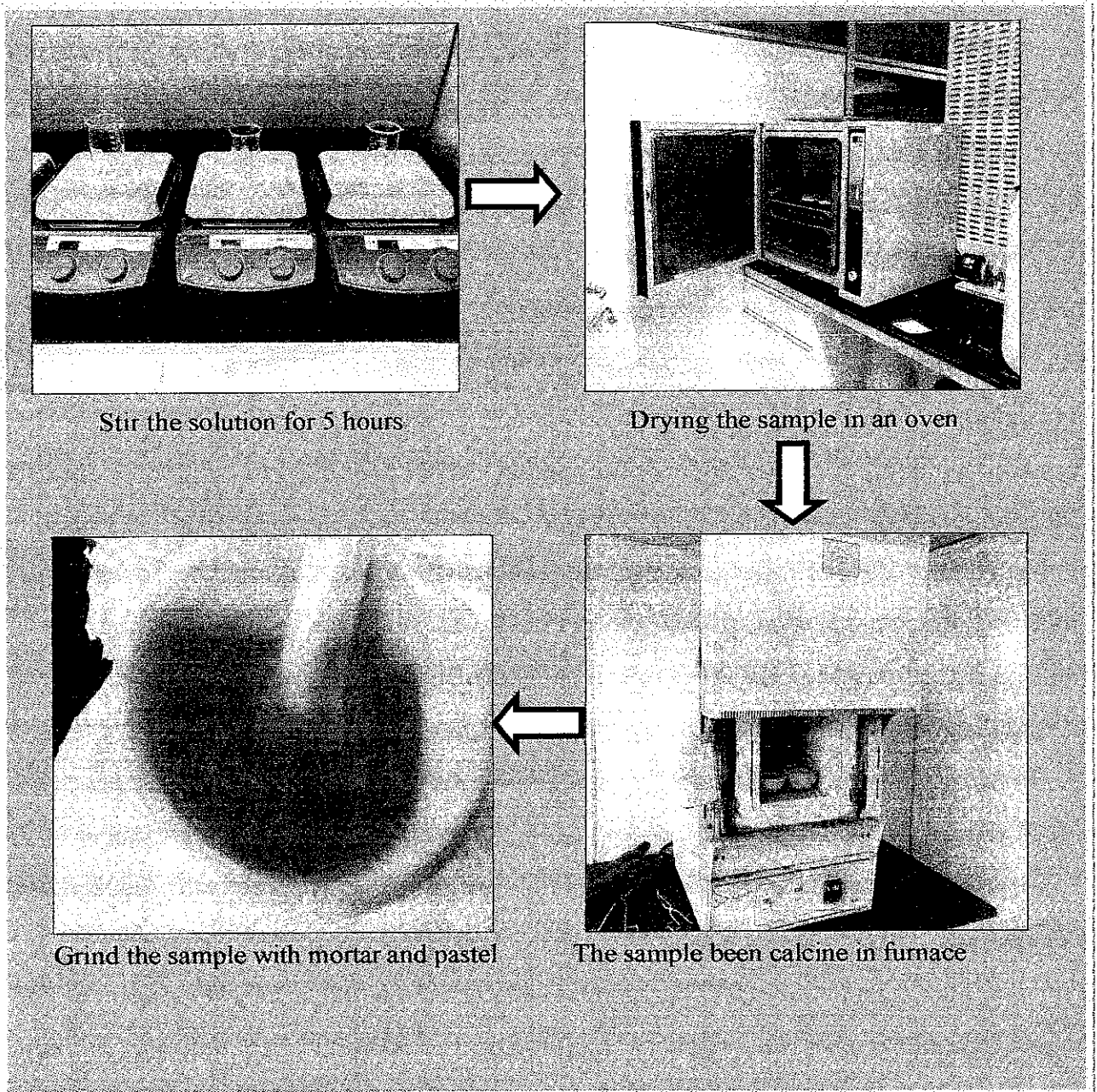


Figure 3.5: Preparation of 5wt% Fe/SiO₂ using impregnation method

4.0 RESULTS & DISCUSSION

4.1 Silica preparation

The attempts to do a silica sphere support for iron catalyst has failed due to several causes such as contaminated and change of final silica color. There have been four attempts to do a silica support before the fifth attempt has end up with a success. There are many variables that need to be control such as speed of stirring, cleanliness of equipment and glassware, chemicals that have been contaminated and so on. The first three attempts have been failed when the color of silica was changed from pure white to purple and brownish respectively. The fourth attempt the color of silica is pure white but the BET result is not like the desired one where the BET is $198\text{m}^2/\text{g}$ instead of less than $100\text{m}^2/\text{g}$. The final attempt was successful where the color of the silica sphere is pure white and the BET is less than $100\text{m}^2/\text{g}$ where after characterize it the sample has a bet of $61\text{m}^2/\text{g}$.

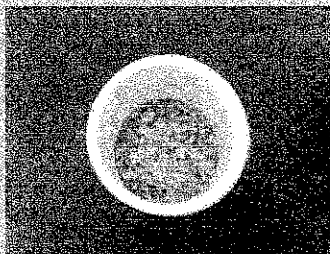
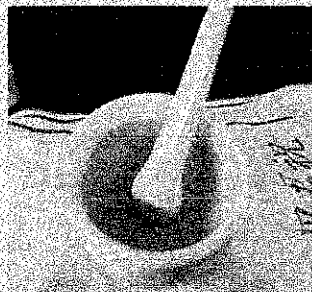
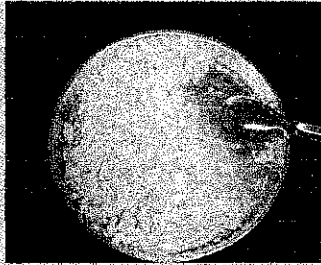
During the final attempt in preparing the silica the author has been in extra precaution with the cleanliness of the equipment and glassware. The author follows the methodology continuously until when we want to put the solution in the oven after finish doing rotary evaporator. Instead put the sample in one patry disc the author put the sample into two discs separately. Same goes when placing the sample into furnace for calcinations. The author has put the sample into two crucibles that have been cleaned before with high temperature. The empty crucibles were put in the furnace overnight at 550°C to remove all particles that might had at the surface of crucibles.

The summary of attempts preparing a silica sphere support is shown as below:

Attempt	Final Weight (g)	Observation	Analysis
1	16.4383	The silica color changed from pure white to purple after going out from the furnace. Expected the sample have been overheated or contaminated.	Samples have been contaminated because the cover of crucibles not been removed while calcinations. Results failed.
2	14.308	The silica color changed from pure white to dark brownish after going out from the furnace.	Samples have been contaminated because of the crucibles. Results failed.
3	12.265	When stirring the solution in the beaker it was not been covered with parafilm. The solution was drastically decreased in terms of volume. The silica changed color to light brownish. The top part of the silica is pure white but the bottom part was contaminated.	The samples have again been contaminated even the crucibles were changed with another type of crucibles. A chemical [Tetraethyl ortosilicate (TEOS)] is suspected to be contaminated because have been kept for too long period. Results failed.
4	13.456	The samples are clearly pure white after been calcined. The samples have been put into two different crucibles to maximize the calcinations to remove impurities.	The samples have been sent for BET analysis. Unfortunately the results show that the BET is 198 which larger than maximum allowable BET, 100. It is suspected come from the speed when stir because the stirring rate is too fast. Results failed.

5	14.1373	The samples are clearly pure white after been calcined. No sign of contaminated.	The samples have been sent for BET surface area analysis. The result has come out and the reading is $61.8923\text{m}^3/\text{g}$ Results is a success. The sample of silica sphere can be use to prepare a catalyst.
---	---------	--	---

Table 4.1: Summary of preparing a silica support spheres.

Attempt	Color	Results	Photo
1	Purple	Contaminated. Failed	
2	Dark Brownish	Contaminated. Failed	
3	Light Brownish	Contaminated. Failed	

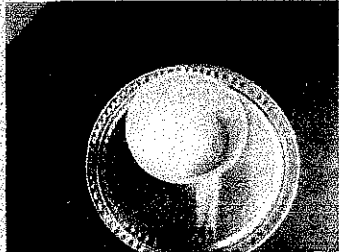
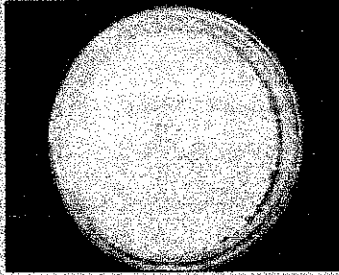
4	Pure White	BET surface area is more than 100. Failed	
5	Pure White	BET surface area is 61.8923m ³ /g. Success	

Table 4.2: *Summary of silica spheres photograph*

It takes almost two months to prepare and characterize the silica support before the author can proceed to the next step which is to prepare iron catalyst. After characterizing the BET surface area, the result is as follows:



Figure 4.1: *The isotherm plot on silica spheres*

Adsorption isotherms can be classified in six types according to IUPAC^[26]. The type I is typical for micro porous solids and chemisorptions isotherms. Type II is shown by finely divided non-porous solids. Type III and Type V are typical of vapors. Type IV and Type V feature a hysteresis loop generated by the capillary condensation in mesopores. The rare Type VI, the steps-like isotherm is shown with nitrogen on special carbons. The graph above is the Type II of adsorption isotherms where it indicate a finely divided non-porous. The types of graph above can be compared with the rest of adsorption isotherms.

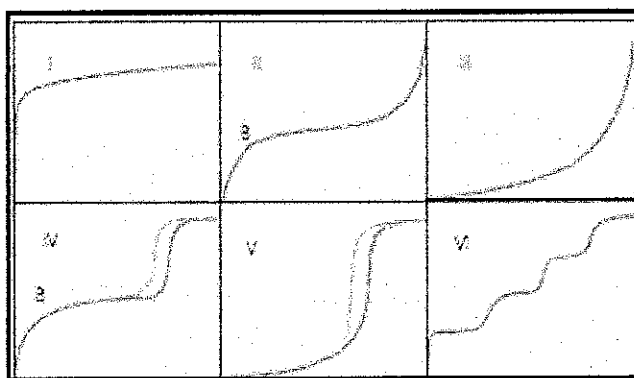
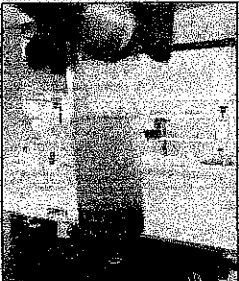


Figure 4.2: *Adsorption isotherms*^[27]

4.2 Catalyst preparation (Ammonia Method)

The author has followed the methodology that has been prepared (Chapter 3). For ammonia deposition the author have been used an overhead stirrer to stir the solutions of $\text{Fe}(\text{NO}_3)_3 \cdot 9\text{H}_2\text{O}$ and silica. The author decide to put 0.5g of silica to add into 0.19g of $\text{Fe}(\text{NO}_3)_3 \cdot 9\text{H}_2\text{O}$. The speed of overhead stirrer is fixed at 200rpm. The author has doing a 5wt% of Fe/SiO_2 loading first then follow by 3wt% and 2wt% respectively. Different loading will result a different weight of $\text{Fe}(\text{NO}_3)_3 \cdot 9\text{H}_2\text{O}$ that will add into solution.

Methodology (in sequence)	Photo	Observation
After Stir		There were three layers inside it contains a very darker brownish layer, brownish layer and water layer. There is also a tiny white layer at the bottom of it.
After Centrifuge		The layers were more clear after the sample been centrifuge. At the bottom there is still a tiny layer of white color suspected is silica, the middle layer is an iron layer while at the top is a clear water layer.
After Filter		The iron catalyst is a brownish in color. The sample is separated into small pieces by washing it with water.

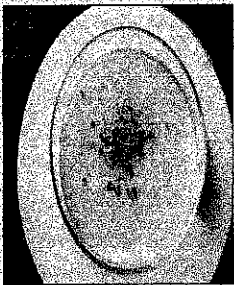
<p>After Drying</p>		<p>After drying the sample overnight plus with 3 more hours in an oven the sample color change to more bright brownish. Some of the pieces were brown n color and some are white which shows that it not well distributed.</p>
<p>During and After Grinding</p>		<p>After grinding the color of the sample become darker and it changed into powder form.</p>

Table 4.3: Summary of observation of ammonia deposition method.

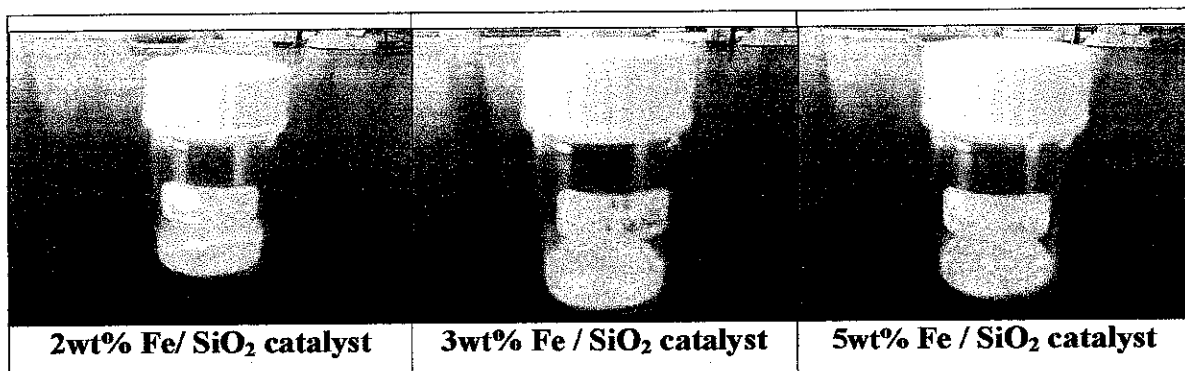


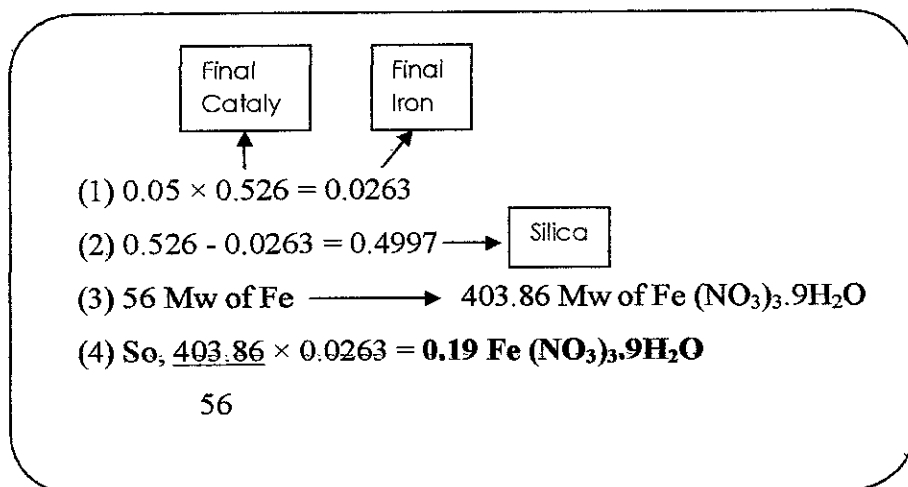
Figure 4.3: Comparing the color of different loading of Fe / SiO₂ catalyst

As shown in *Figure 4.4* above, different metal loading will result different catalyst color. As it goes the lower metal loading which is 2wt% Fe / SiO₂ has a brightest brownish color compared to higher metal loading which is 5wt% Fe/ SiO₂ has a darker brownish color. So it shows that the higher metal loading of the catalyst, the more darkly the color will be. This can happen due to addition of metal inside the solution before stirring it where it depends on the calculation. The calculation is based on ratio of

iron and silica itself where it figure out by trial and error method. The sample of calculation of 5wt% Fe/ SiO₂ is shown as below:

4.2.1 Catalyst calculation (5wt% Fe/ SiO₂):

Assume silica to be 0.5grams.



Metal Loading	Weight of Fe (NO ₃) ₃ .9H ₂ O (grams)
2wt%	0.074
3wt%	0.11
5wt%	0.19

Table 4.4: Summary of metal loading and weight of iron

After all the catalyst from different metal loading have been prepared, the sample is sending for characterization of Scanning Electron Microscope (SEM) and Xray Diffraction (XRD). Here are the photographs that have taken from SEM equipment and the analysis from Energy Dispersive X-ray (EDX) for 5wt% Fe / SiO₂ ammonia deposition method.

4.2.2 SEM and EDX characterization

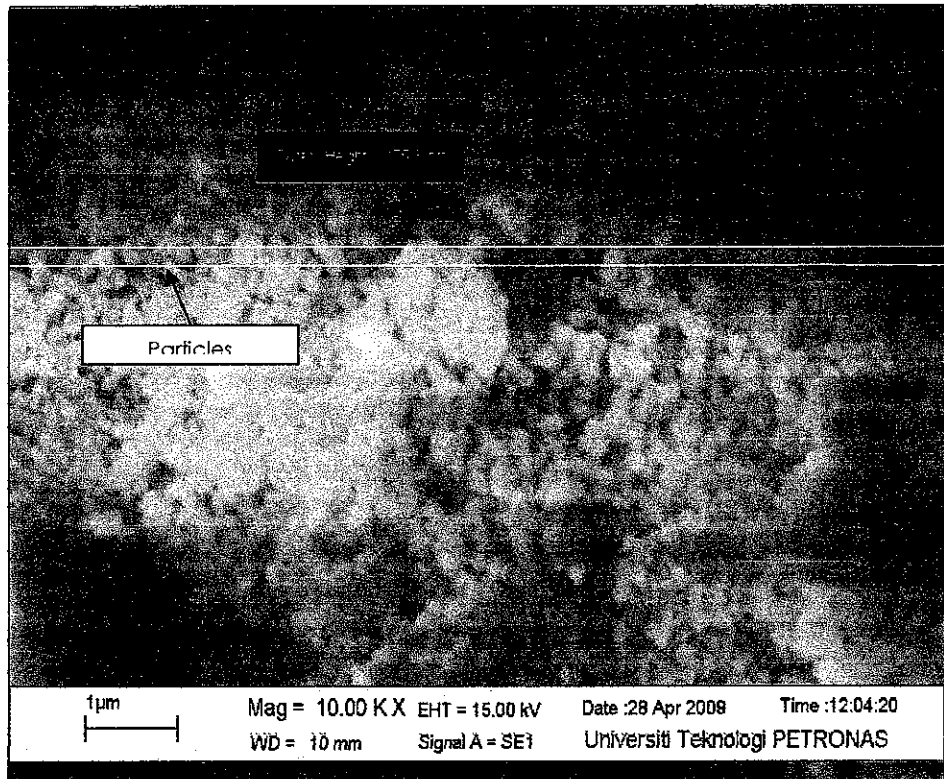


Figure 4.4: Scanning Electron Microscope image of 5wt% Fe / SiO₂ loading

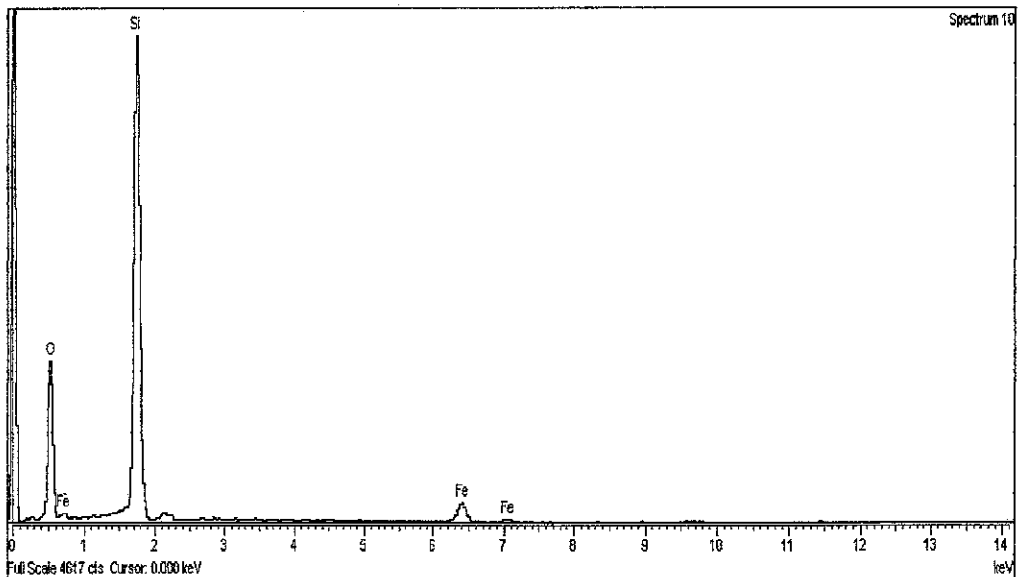


Figure 4.5: The composition graph of 5wt% Fe / SiO₂ loading

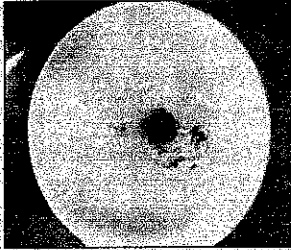
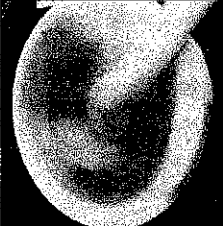
Figure 4.4 and 4.5 shows the results of SEM and EDX respectively. From the image of SEM we can say that the silica is spherical in shape. From the graph above we can confirm that there are only three components exist in the catalyst which is iron (Fe), silica (Si) and oxygen (O). The graph shows that this catalyst a very large amount of silica and very small weight of iron. The composition and weight of all three particles as shown below:

Element	Weight %	Atomic %
Oxygen	52.27	71.30
Silica	38.21	27.09
Ferum	4.52	1.61

The weight % of ferum is 4.52 which show that it is near to 5wt% that have been selected before. For now, only 5wt% of Fe / SiO₂ can be done due to limitation. After this the author will continue to characterize for 2wt% and 3wt% of the sample.

4.3 Catalyst preparation (Impregnation Method)

This methodology is same with ammonia deposition where the author had started with highest loading first which is 5wt% of loading. The author will continue with 3wt% and 2wt% of loading the next day respectively.

Methodology (in sequence)	Photo	Observation
Stirring		Some of the solution has been evaporated to the air. Some of the part has changed to solid and some other part still has water.
Filter	-	The solid part was left as a sample. The color becomes yellowish.
Drying	-	The solid become brownish.
After Heating		The sample becomes darker in color.
Grind		The color become less dark than previous due to particles is not well distributed.

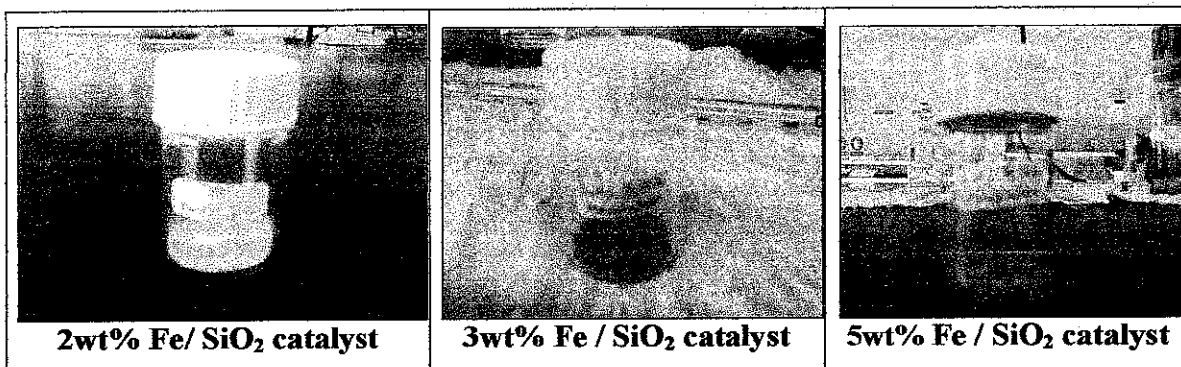


Figure 4.6: Comparing the color of different loading of Fe / SiO₂ catalyst

As shown in *Figure 4.7* above, different metal loading will result different catalyst color. As it goes the lower metal loading which is 2wt% Fe / SiO₂ has a brightest brownish color compared to higher metal loading which is 5wt% Fe / SiO₂ has a darker brownish color. So it shows that the higher metal loading of the catalyst, the more darkly the color will be.

4.3.1 SEM and EDX characterization

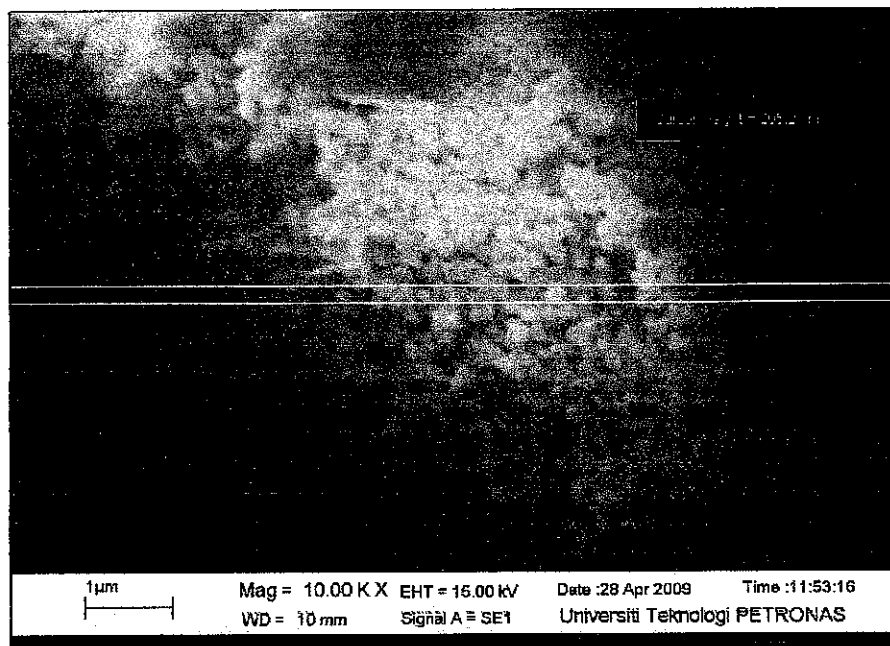


Figure 4.7: Scanning Electron Microscope image of 5wt% Fe / SiO₂ loading

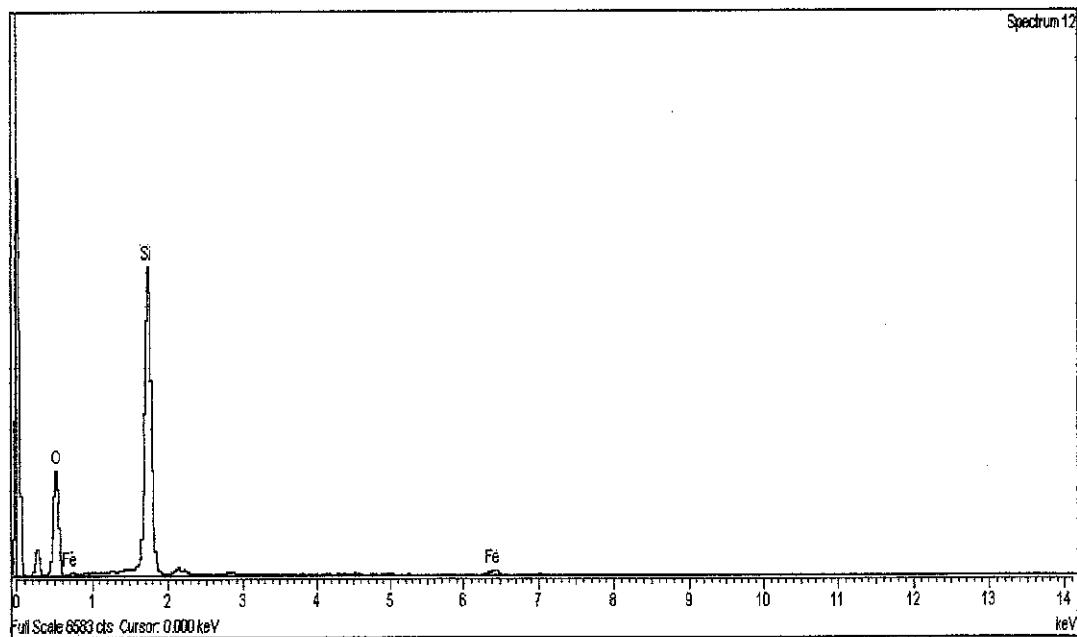


Figure 4.8: The composition graph of 5wt% Fe / SiO₂ loading

Figure 4.7 and 4.8 shows the results of SEM and EDX respectively. From the image of SEM we can say that the silica is spherical in shape. For impregnation method the image looks agglomerated and the cause of this scenario happens when the author calcines the sample in the furnace where the thermal effect occurs. From the graph above we can confirm that there are only three components exist in the catalyst which are iron (Fe), silica (Si) and oxygen (O). The graph shows that this catalyst has a very large amount of silica and a very small weight of iron. The composition and weight of all three particles are shown below:

Element	Weight %	Atomic %
Oxygen	60.70	73.51
Silica	37.49	25.87
Iron	1.81	0.63

The weight % of iron is 1.81 which shows that it is far from 5wt% that has been selected before. For now, only 5wt% of Fe / SiO₂ can be done due to limitation. After this the author will continue to characterize for 2wt% and 3wt% of the sample.

4.3.2 Transmission Electron Microscope (TEM)

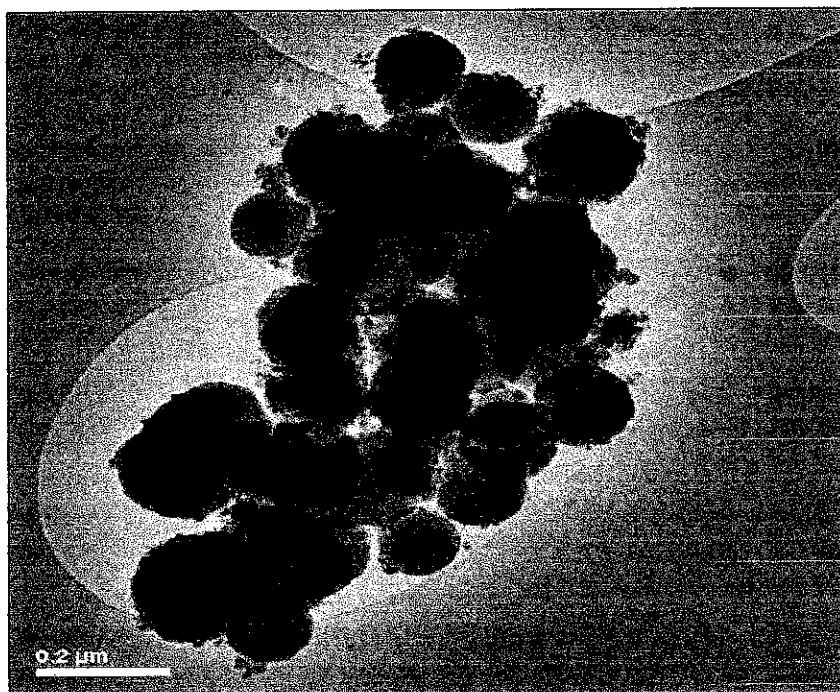


Figure 4.9: *Transmission Electron Microscopy (TEM) image of the synthesized silica spheres*

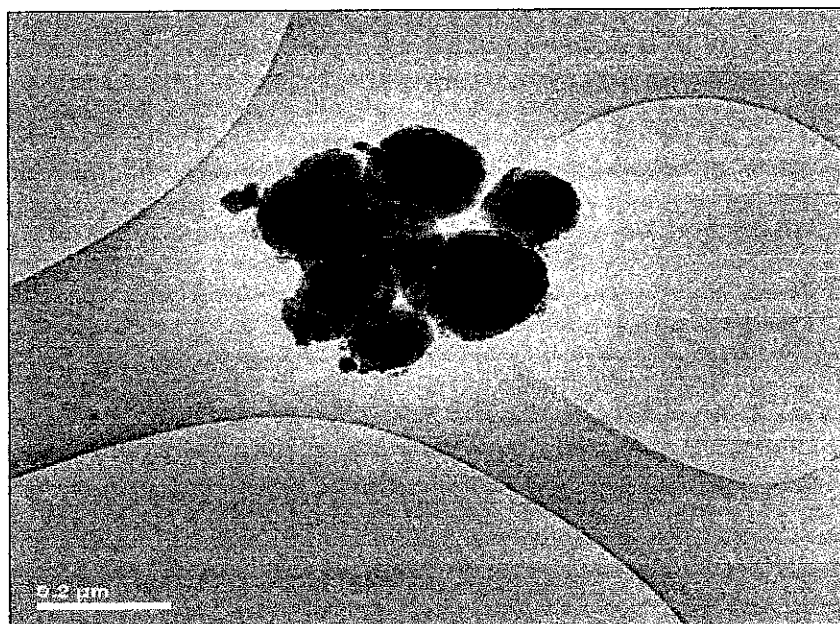


Figure 4.10: *Transmission Electron Microscopy (TEM) image of the synthesized silica spheres*

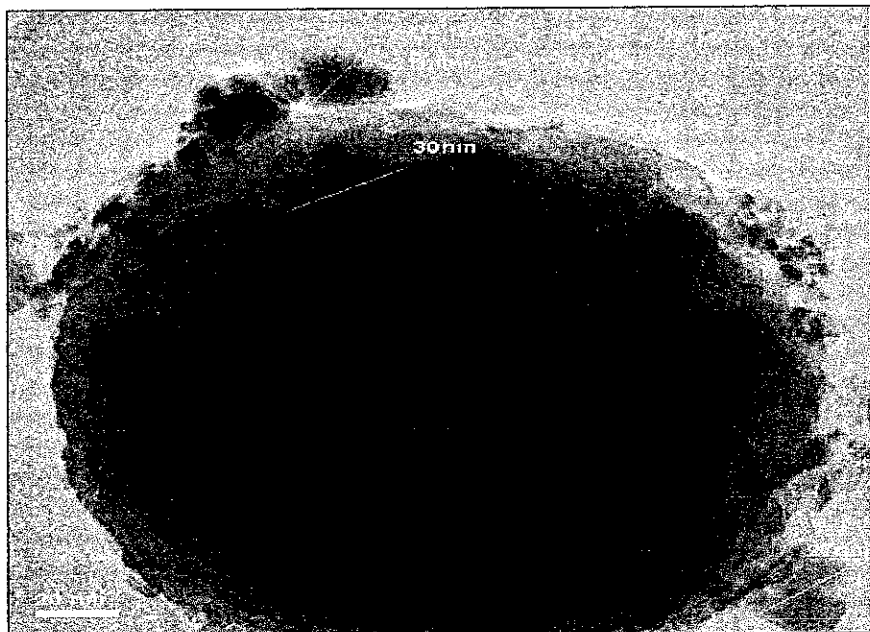


Figure 4.11: *Transmission Electron Microscopy (TEM) image of 5wt% Fe/SiO₂ Catalyst of impregnation method*

From figure 4.9 and 4.10 shows TEM images of the synthesized silica spheres. The silica spheres were considered nonporous and smooth surface with slightly sharp edges. The average diameter of each silica spheres is at 168nm. Figure 4.11 shows the TEM image of the 5wt% Fe/SiO₂ spherical model (Fe-21nm) catalyst prepared by impregnation, which is, mixing a iron nitrate solution with the nonporous silica spheres followed by drying and calcinations. The catalyst model was found to be well-defined with proper attachment of iron metal on the silica spheres. However, it seems that the iron particle size is bigger than expected (12nm).

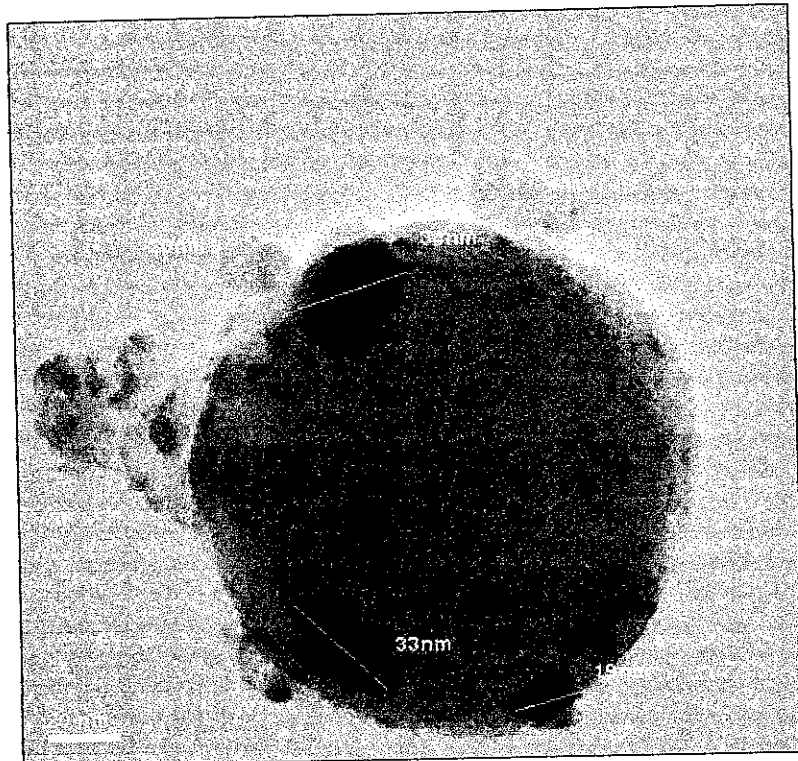


Figure 4.12: TEM image of 5wt% Fe/SiO₂ catalyst with different iron size attached on the silica

From Figure 4.12 above shows that iron particles at different size attached on the silica sphere of 5wt% Fe/SiO₂. It shows the size of iron metal attached on the particle is in range of 19nm-34nm. The range is too big whereas the desired range of iron metal is below 12nm. In the figure shows the distribution of iron metal is inconsistencies on the support. This might be because of unevenly stirring of mixture during the catalyst preparations where the solution may not be contact at all area. The stirring process was not uniform throughout the mixture, causing only certain amount of iron particles mixed with the silica spheres.

4.3.3 X-ray Diffraction (XRD)

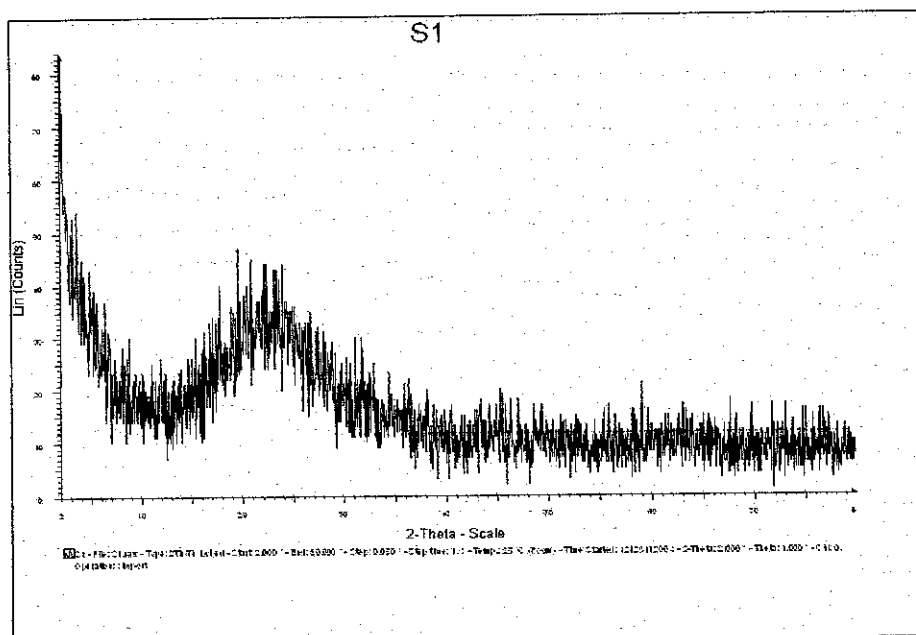


Figure 4.13: XRD result for 3wt% Fe/SiO₂ catalyst by impregnation

Figure 4.13 shows the representation of amorphous nature of the 3wt% Fe/SiO₂ catalyst after XRD analysis. For 3wt% of iron loading we know that the supported catalyst is largely covered with silica which contains only 3% makes it hard for the catalyst to be in crystalline structure. An amorphous solid is the kind in which there is no long chain order of the position of the atoms. Theoretically, given a sufficiently high cooling rate, any liquid can be made into amorphous solid. It is difficult to make a distinction between truly amorphous solids and crystalline solids if the size of the crystals is very small. Even amorphous materials have some short-range order at the atomic length scale due the nature of chemical bonding. Furthermore, in very small crystals a large fraction of the atoms are located at or near the surface of the crystal; relaxation of the surface and interfacial effects distort the atomic positions, decreasing the structural order.

4.4 Comparison of Impregnation Method and Ammonia Deposition Method

Theoretically, iron catalyst will react well in impregnation method compare to deposition method. Looking at the image in Figure 4.5 and 4.8 the author can say that the image just can tell about the shape of silica which sphere. The impregnation method image look agglomerated maybe because of the lense of SEM equipment that touch the sample make the sample look like that. It also maybe because the image is just takes at one spot of the catalyst where the result may not that accurate.

Looking at EDX results it shows that ammonia deposition is better for iron compared to impregnation method although the theory tell otherwise. This result is only base on 5wt% for both methods so when the author can managed to get the result for 2wt% and 3wt% samples, the author can get the accurate result.

5.0 CONCLUSION AND RECOMMENDATIONS

The author has desired result for silica sphere after the 5th attempt when the color of the silica is pure white and the BET is less than 100 where the result is 61.8923 m²/g. The reason for the previous result has been failed is because there were some parameter that the author has missed looked such as the cleanliness of the crucibles and the speed when stirring the solution. In the end, after understand all the problems the author has managed to get a desired silica support. So it shows that a silica spheres can be made to achieve the first objective.

For the iron catalyst, after the result of scanning electron microscope (SEM) and Energy Dispersive Xray (EDX) for 5wt% Fe / SiO₂ catalyst has come out, the author found out that the ammonia deposition method is more preferable for iron catalyst compared to impregnation method. The conclusion is made base on the result that has shown from the image of SEM and the weight % of element at EDX for 5wt% of Fe / SiO₂. After this, the author will continue to characterize the sample from 2wt% and 3wt% and hopefully from there an accurate and correct result will appeared.

Transmission Electron Microscopy (TEM) analysis conducted on sample of 5wt% Fe/SiO₂ catalyst by impregnation method yield an estimated average of iron particles with 25nm diameter attached on a silica sphere. X-ray Diffraction (XRD) measurement indicated that the catalyst samples are in amorphous state.

There are several recommendations can be made to improve the outcome of this project in the future:

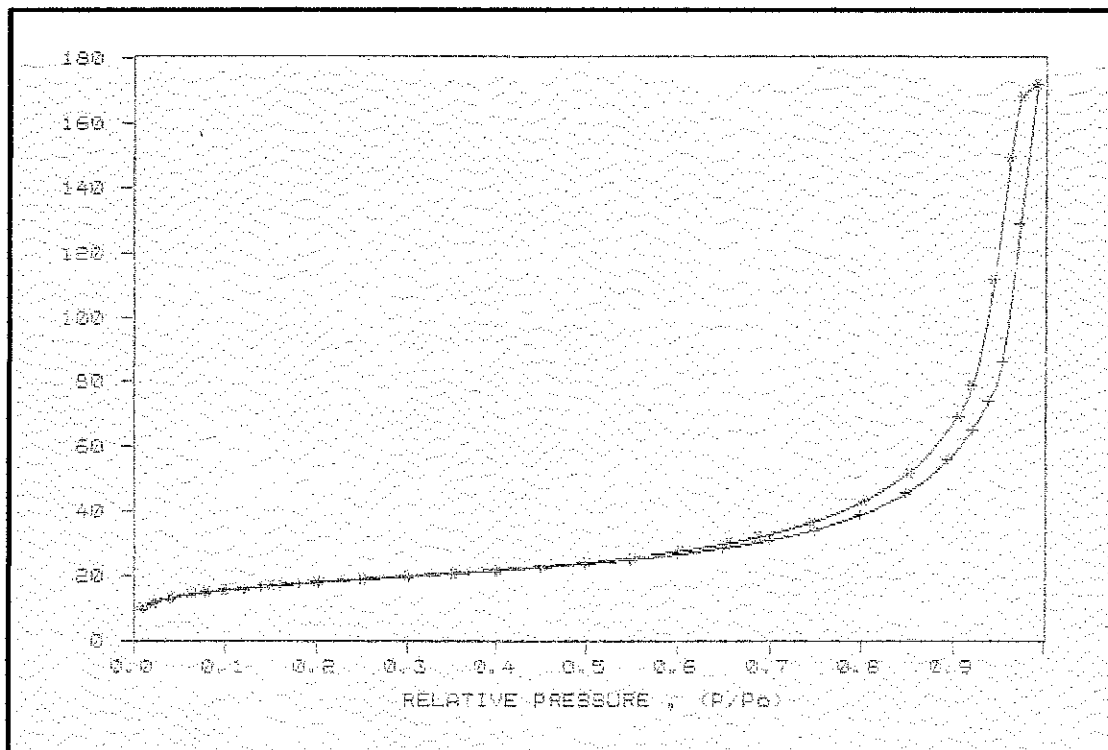
- All the equipments must clean and in good condition when doing the experiment. For example the crucibles use to prepare the silica must be clean to avoid the sample been contaminated.
- The variables such as stirring speed must be fixed and always use the same magnetic hot plate to avoid change of speed.

REFERENCE

- [1] Wiley-VCH Verlag GmbH & Co. KGaA, D-69451 Weinheim. **2005**, 483
- [2] G.B. Sergeev, *Usp. Khim.* **2001**, 70, 915-933
- [3] K.Klabunde in *Nanoscale Materials in Chemistry* (Ed.: K.Klabunde), Wiley-Interscience, New York, **2001**, pp. 1-13.
- [4] C. Kittel, *Phys. Rev.* **1946**, 70, 965–971.
- [5] L. Néel, *C. R. Hebd. Seances Acad. Sci.* **1949**, 228, 664–666.
- [6] C. Bean, J. Livingston, *J. Appl. Phys.* **1959**, 30, 120S–129S.
- [7] I. Jacobs, C. Bean in *Magnetism*, Vol. III (Eds.: G. T. Rado, H.Suhl), Academic Press, New York, **1963**, pp. 271–350.
- [8] G. P. Van der Laan, A. A. C. M. Beenackers, *Catal. Rev. Sci.*
- [9] Wiley-VCH Verlag GmbH & Co. KGaA, D-69451 Weinheim. **2005**, 483-484
- [10] Daage, Michel A. (Baton Rouge, LA), Koveal, Russell John (Baton Rouge, LA), Lapidus, Albert L'vovich (Moscow, RU), Krylova, Alla Jurievna (Moscow, RU), Brennan, Shawn Paul (Baton Rouge, LA). *Fischer-Tropsch catalyst enhancement*. **2002**
- [11] Columbia Electronic Encyclopedia, Sixth Edition, *Fischer-Tropsch Process*. **2008**.
<http://www.answers.com/topic/fischer-tropsch-process>
- [12] Wikipedia, The Free Encyclopedia, *Fischer-Tropsch Process, Original Process*.
www.wikipedia.org
- [13] J.E. Otterstedt and D.A. Brandreth, *Small Particles Technology*, Silica, 1st Edition New York, 30-33, **1998**
- [14] Courtesy Chemical Society of Japan, Goto, **1955**
- [15] J.E. Otterstedt and D.A. Brandreth, *Small Particles Technology*, Silica, 1st Edition New York, Solubility and Particle Size, 32, **1998**
- [16] Boris Imelik, Jacques C. Vedrine, **1992**, "Catalyst Characterization – Physical Techniques for Solid Materials", Plenum Press 510-513

- [17] Wikipedia, Transmission electron microscope.
http://en.wikipedia.org/wiki/Transmission_electron_microscope
- [18] Zhong Lin Wang, 2000, "Characterization of Nanophase Materials", Wiley-VCH. First Edition **2000**, 13-14
- [19] JEOL 840A SEM result, <http://www.unl.edu/CMRAcfem/semout.htm>
- [20] S.J. Gregg, K.S.W. Sing, Adsorption, Surface Area and Porosity, Academic Press, London, 2nd Ed. (**1982**)
- [21] S. Brunauer, L.S. Deming, W.S. Deming and E. Teller, J. Amer. Chem. Soc., **62**, 1723 (**1940**)
- [22] D.H. Everett and J.C. Powl, J. Chem. Soc., Faraday Trans. I, **72**, 619 (1976)
- [23] G. Horvath and K. Kawazoe, J. Chem. Eng. Jap. **16**, 6, 470 (1983)
- [24] W. Stober, A. Fink, E. Bohn, J. Colloid Interface Sci. **26**. **1968**, 62.
- [25] A.M. Saib et al. / Journal of Catalysis **239**. **2006**, 326-339
- [26] IUPAC Reporting physisorption data for gas/solid systems, Pure Appl. Chem., **57**, 603 (**1985**)
- [27] S. Brunauer, L.S. Deming, W.S. Deming and E. Teller, J. Amer. Chem. Soc., **62**, 1723 (**1940**)

APPENDIX A:
BET SURFACE AREA ANALYSIS OF THE SYNTHESIS SILICA
SPHERES

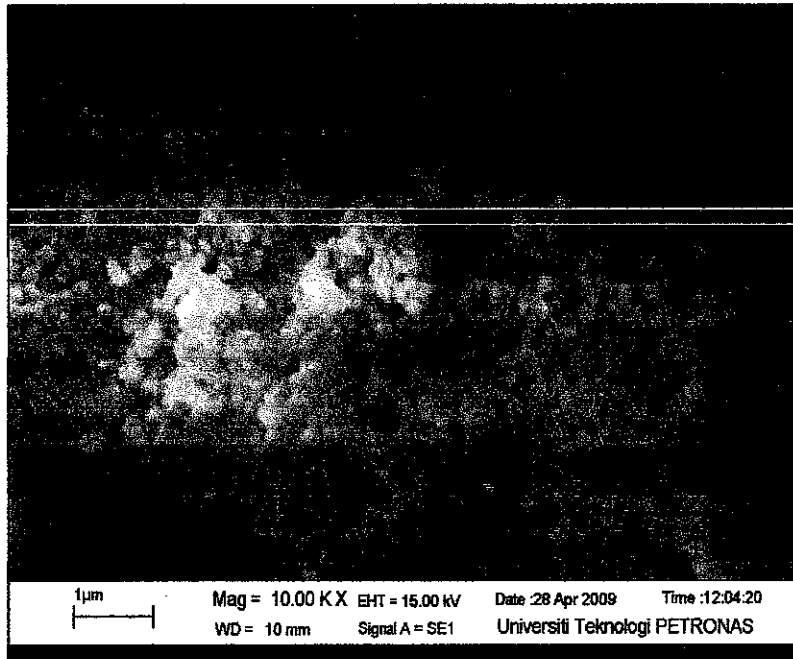


BET SURFACE AREA REPORT

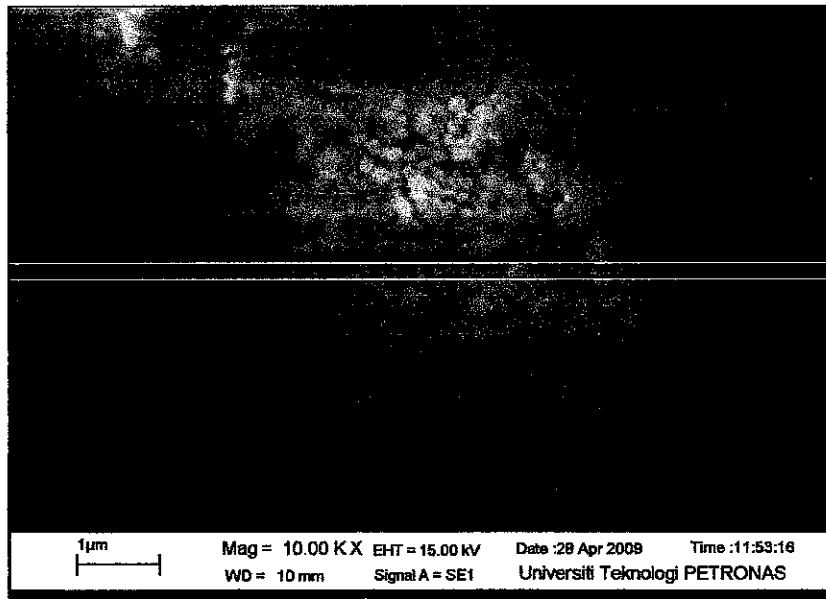
BET SURFACE AREA: 61.8923 +/- 0.9020 sq. m/g
 SLOPE: 0.069939 +/- 0.001024
 Y-INTERCEPT: 0.000396 +/- 0.000052
 C: 177.640060
 VM: 14.217668 cc/g STP
 CORRELATION COEFFICIENT: 9.99679E-01

RELATIVE PRESSURE	VOL ADSORBED (cc/g STP)	1/[VA(Po/P - 1)]
0.0098	9.7306	0.001019
0.0205	11.2564	0.001857
0.0396	12.7508	0.003233
0.0670	14.1205	0.005085
0.0787	14.5700	0.005865

APPENDIX B:
SCANNING ELECTRON MICROSCOPE (SEM) ANALYSIS OF
THE CATALYSTS

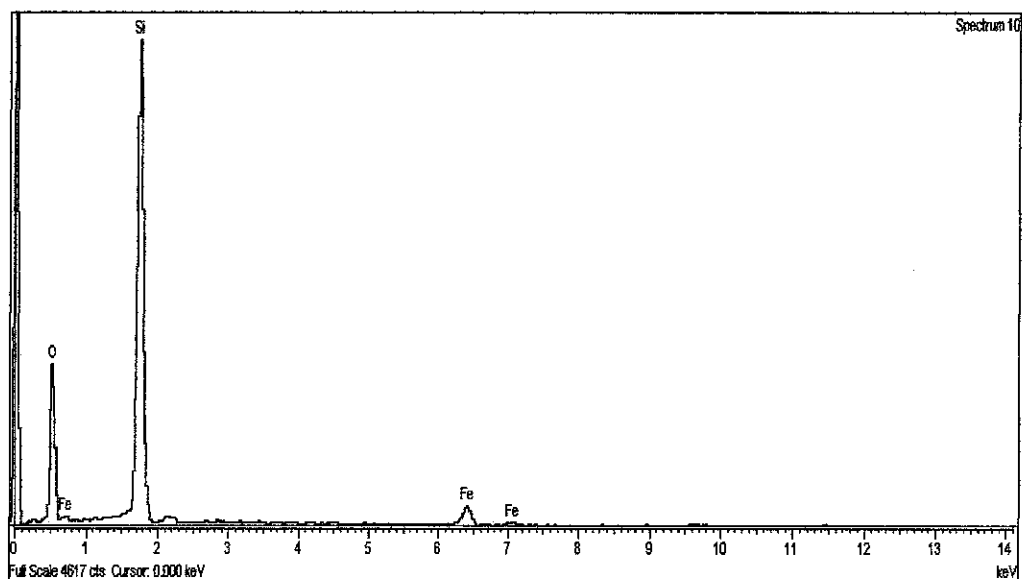


Scanning Electron Microscope image of 5wt% Fe / SiO₂ loading (ammonia deposition)

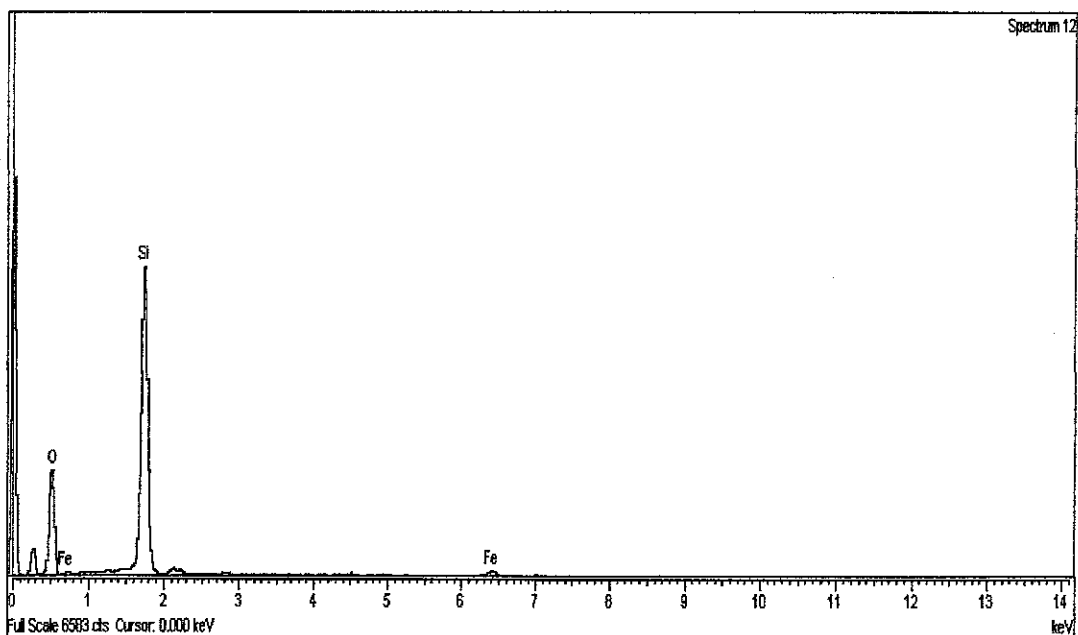


Scanning Electron Microscope image of 5wt% Fe / SiO₂ loading (impregnation)

**APPENDIX C:
ENERGY DISPERSIVE X-RAY (EDX) ANALYSIS OF THE
CATALYSTS**

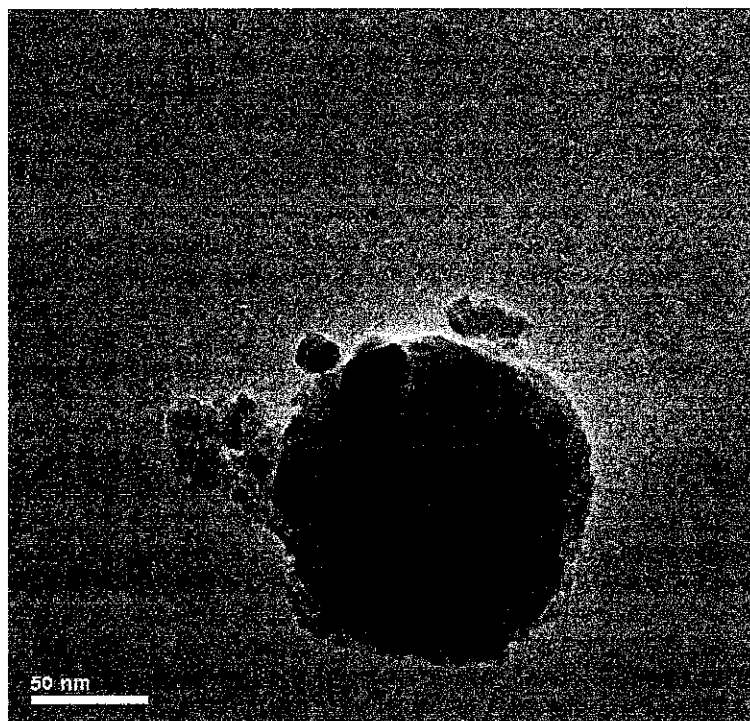


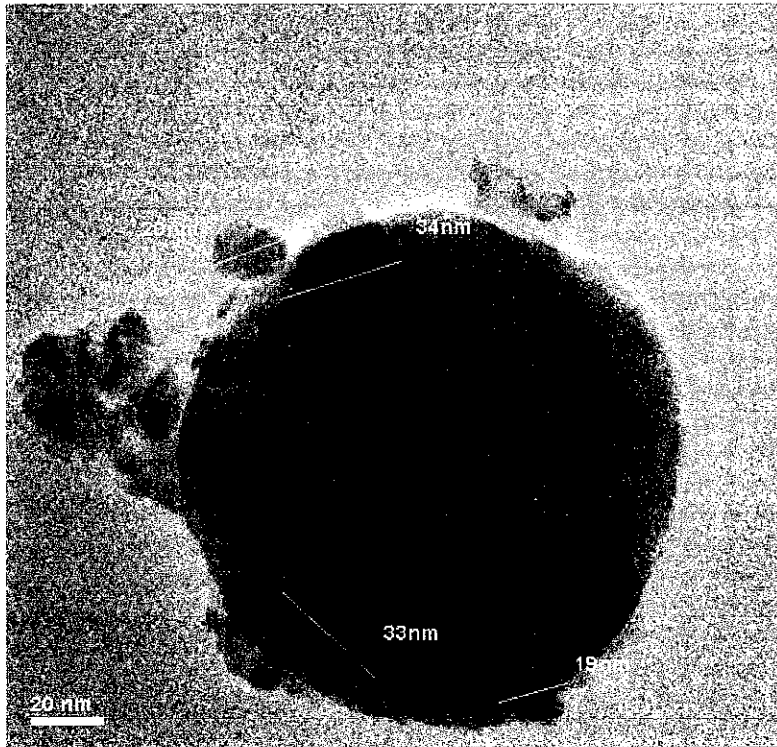
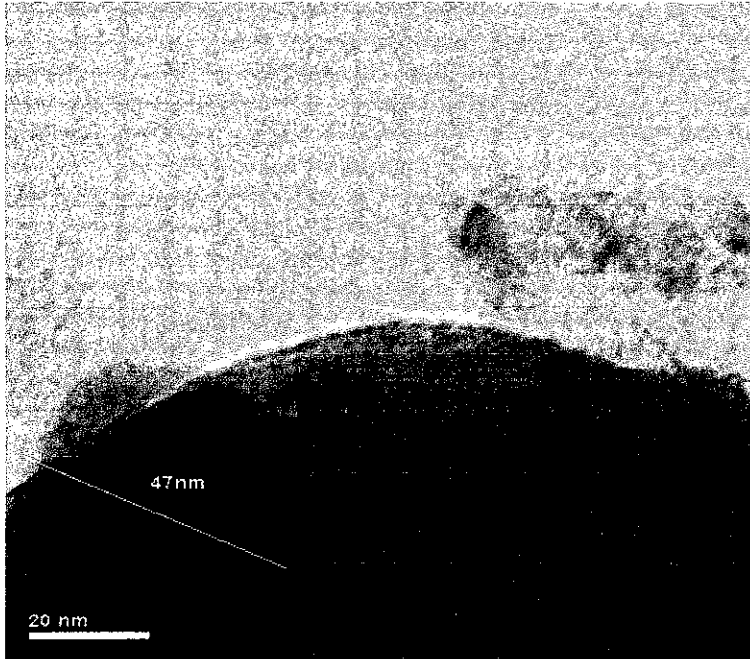
5wt% Fe/SiO₂ catalysts by ammonia deposition method

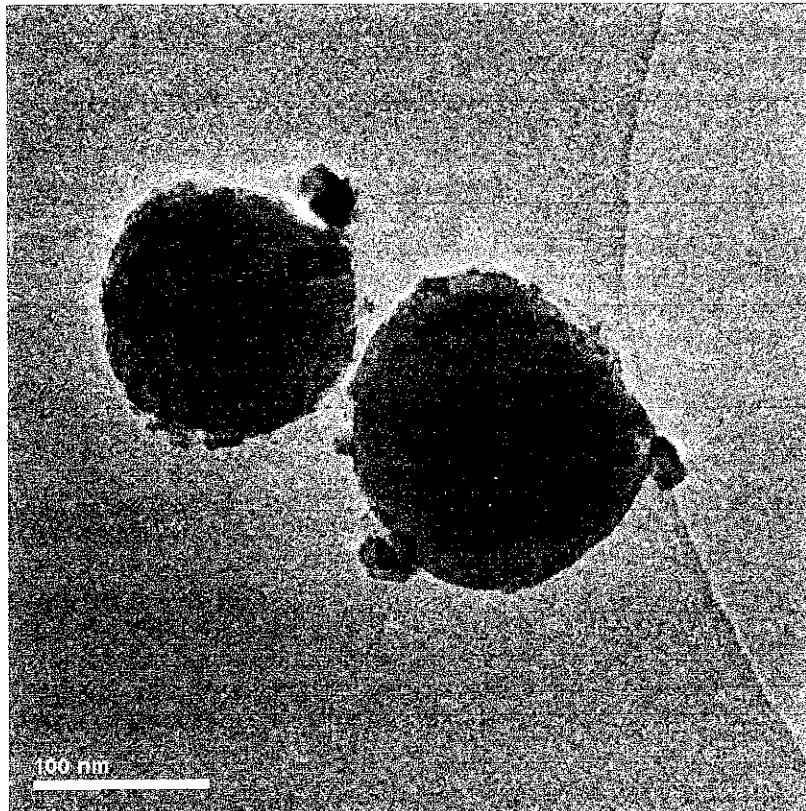
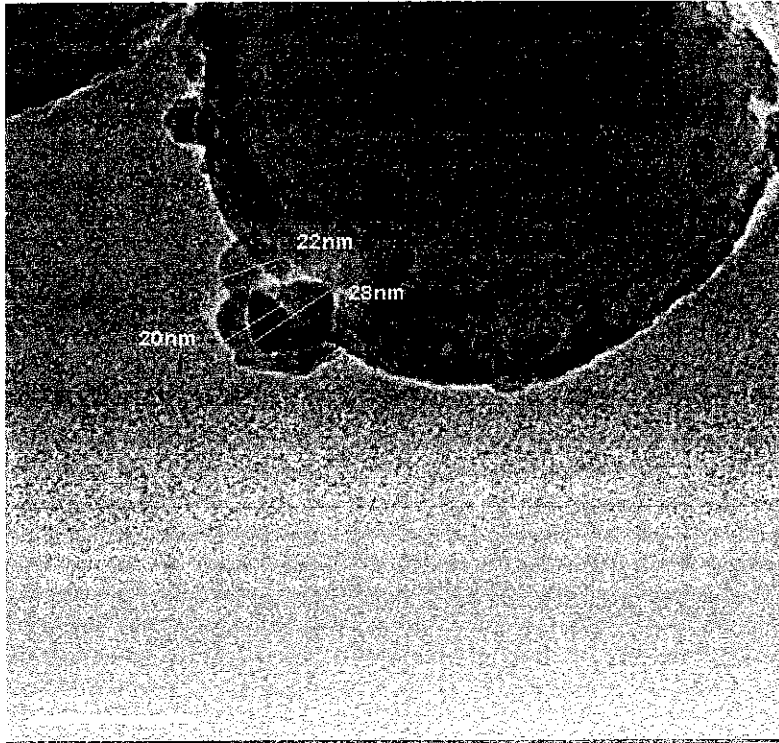


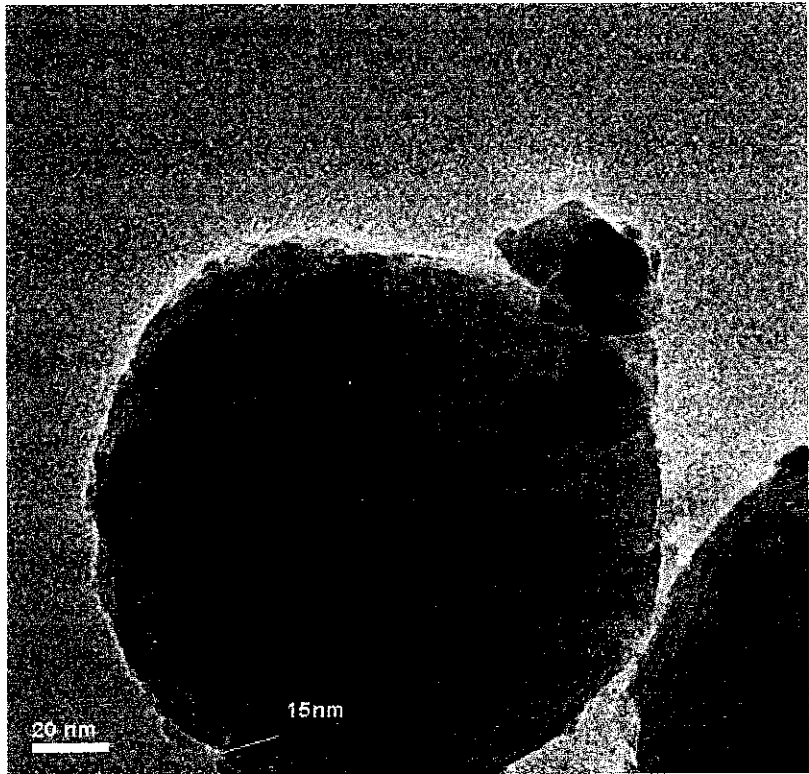
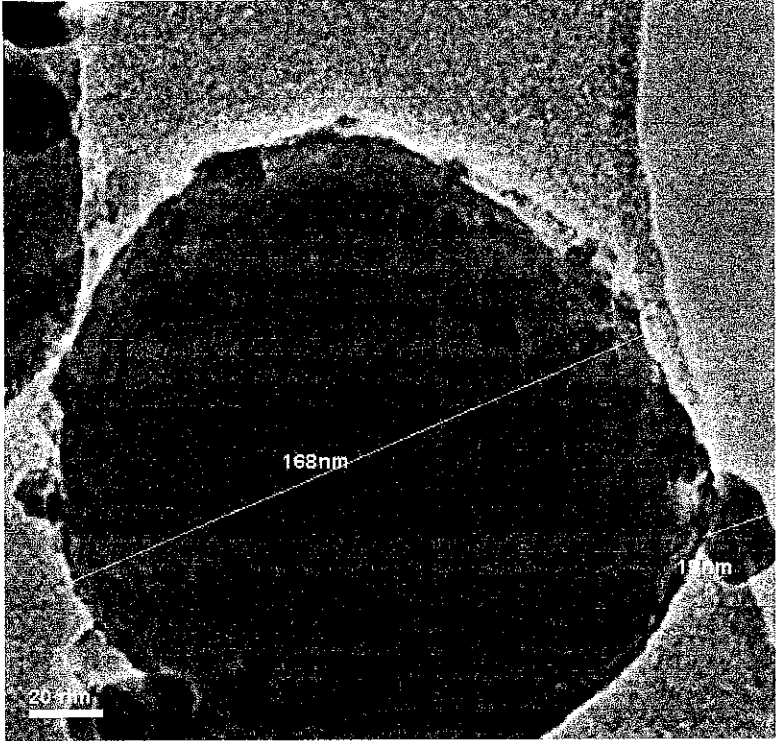
5wt% Fe/SiO₂ catalysts by ammonia impregnation method

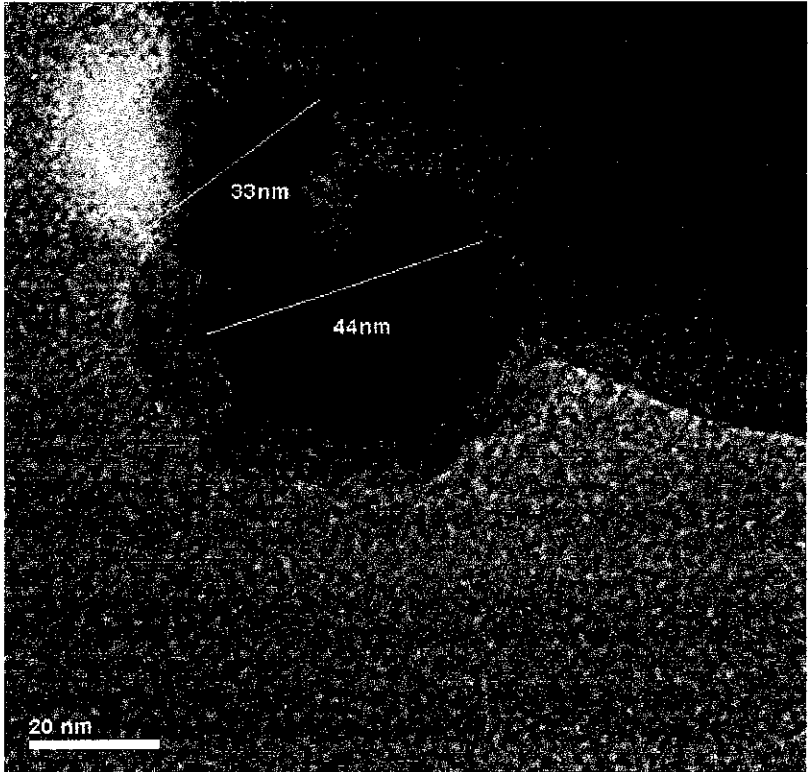
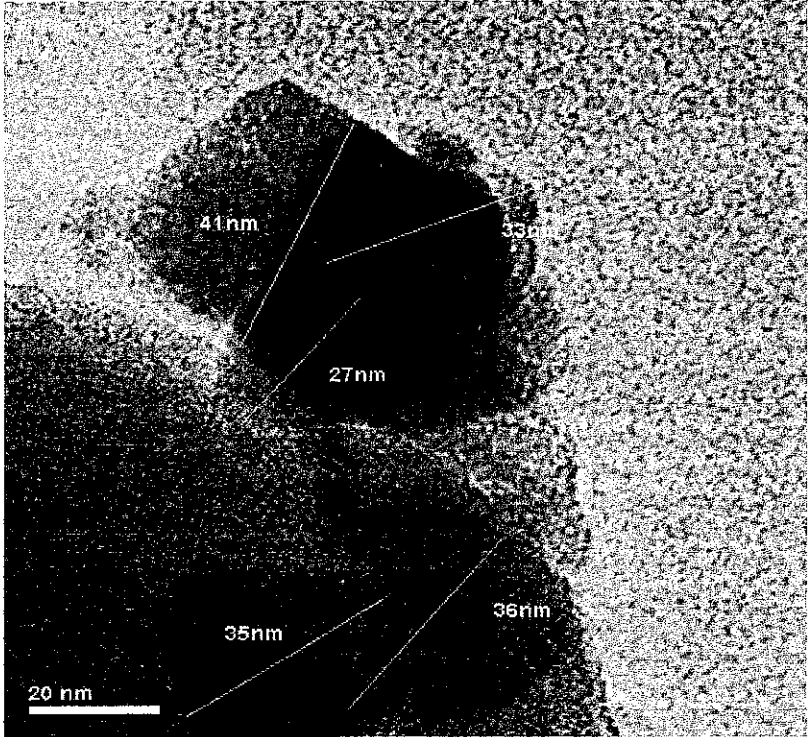
APPENDIX D:
TRANSMISSION ELECTRON MICROSCOPY (TEM) IMAGES OF
5wt% Fe/SiO₂ CATALYST BY IMPREGNATION METHOD

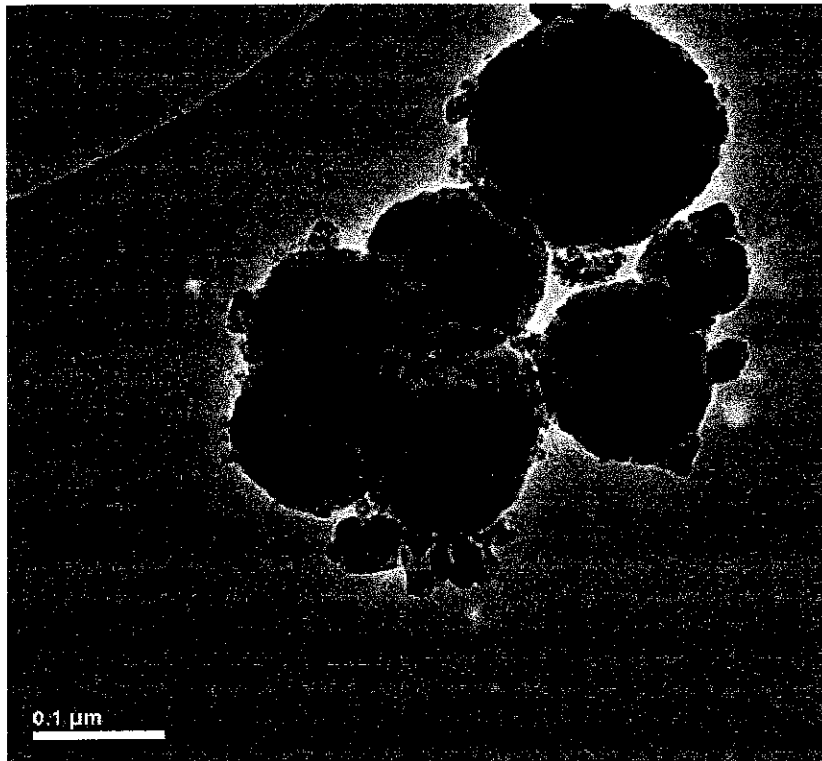
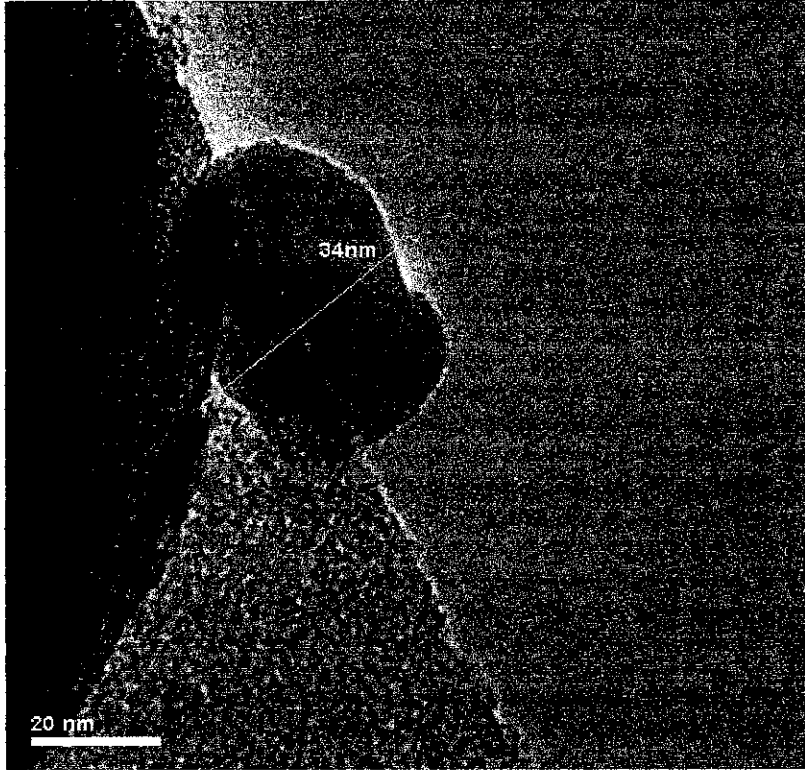


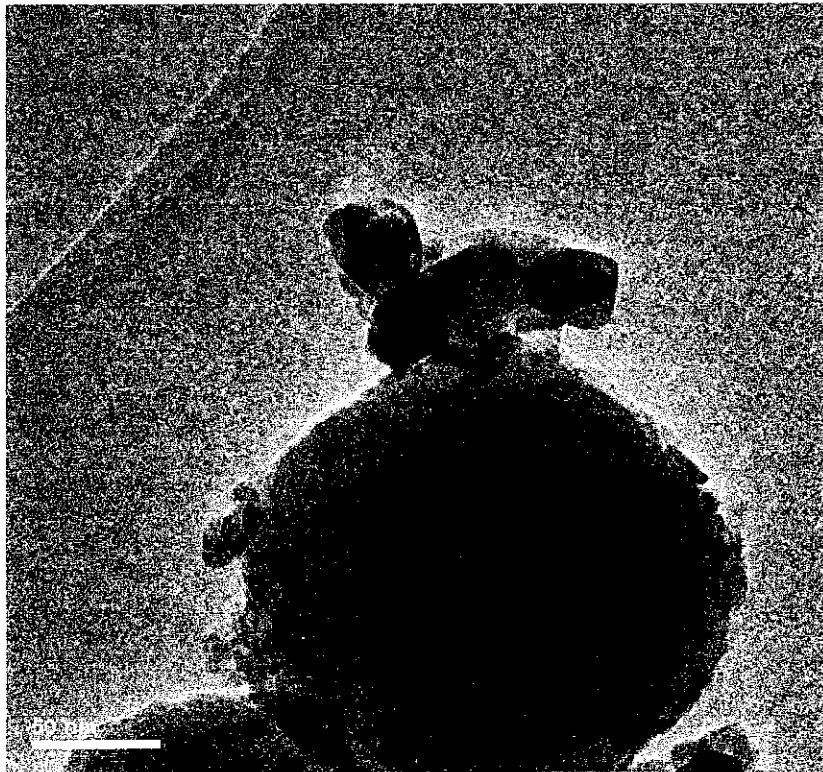
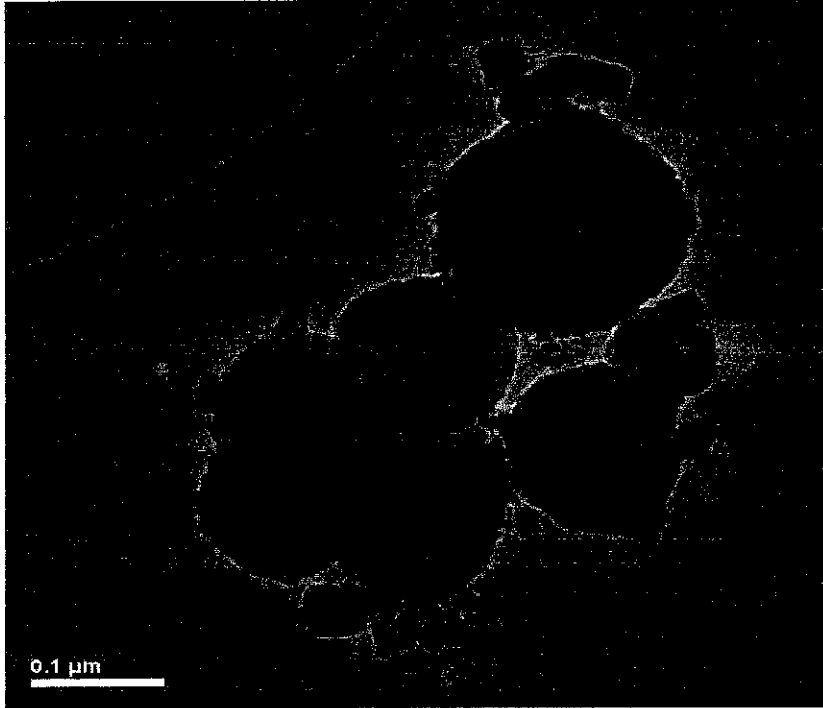


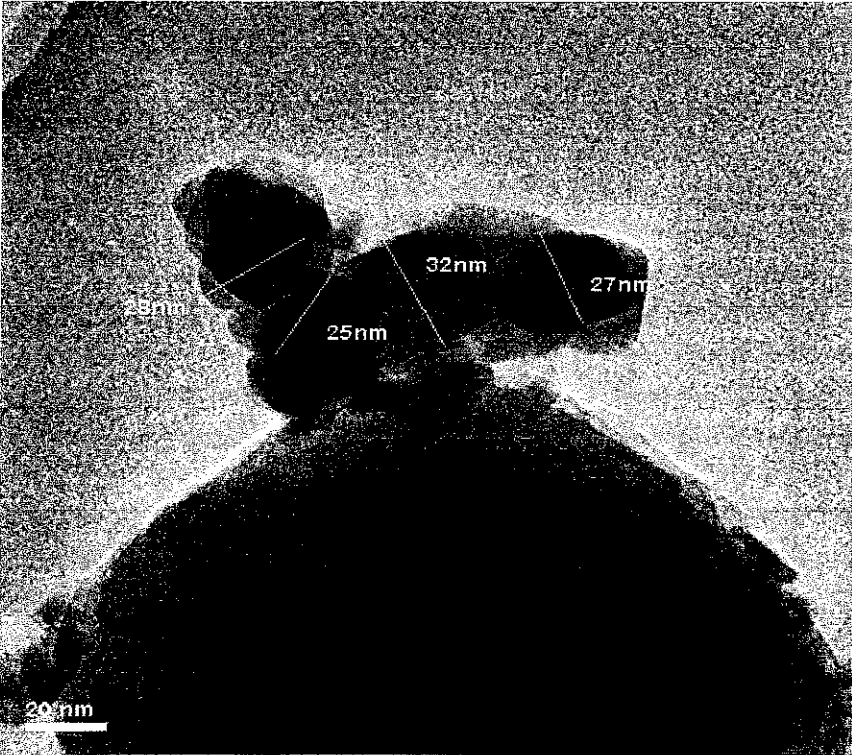
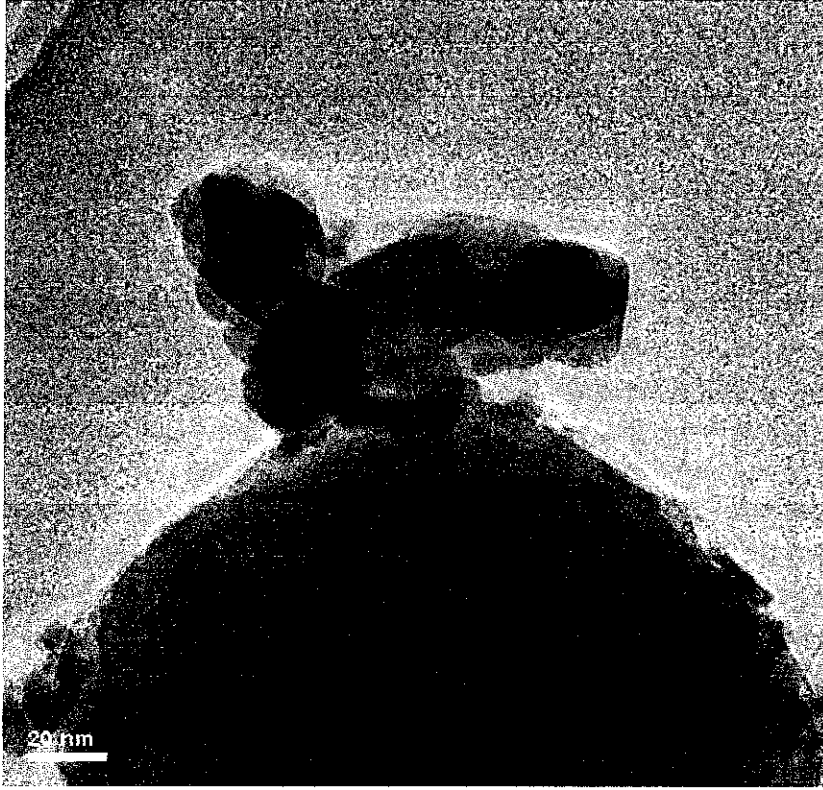


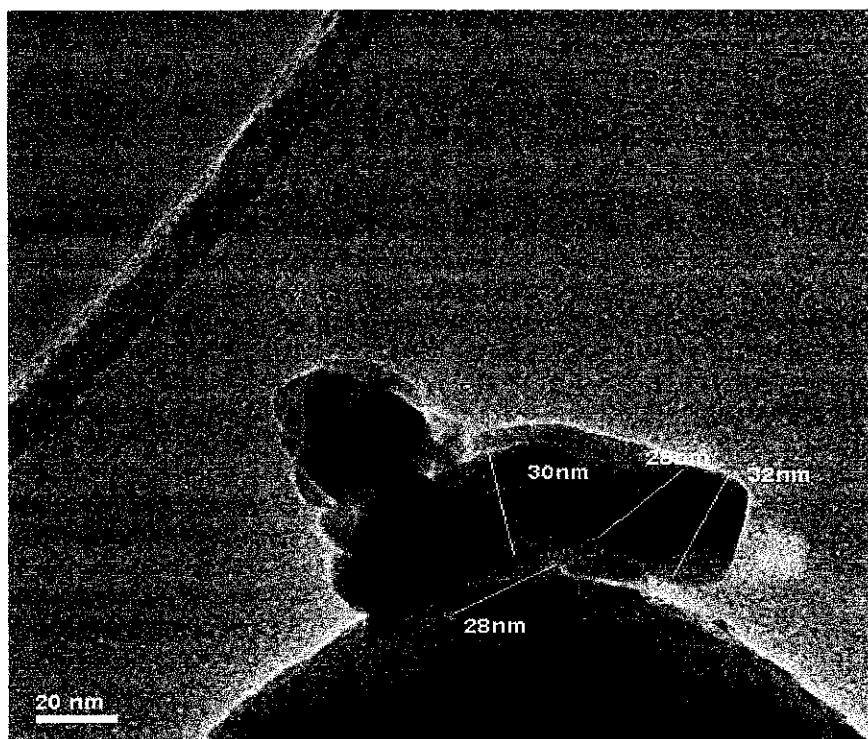
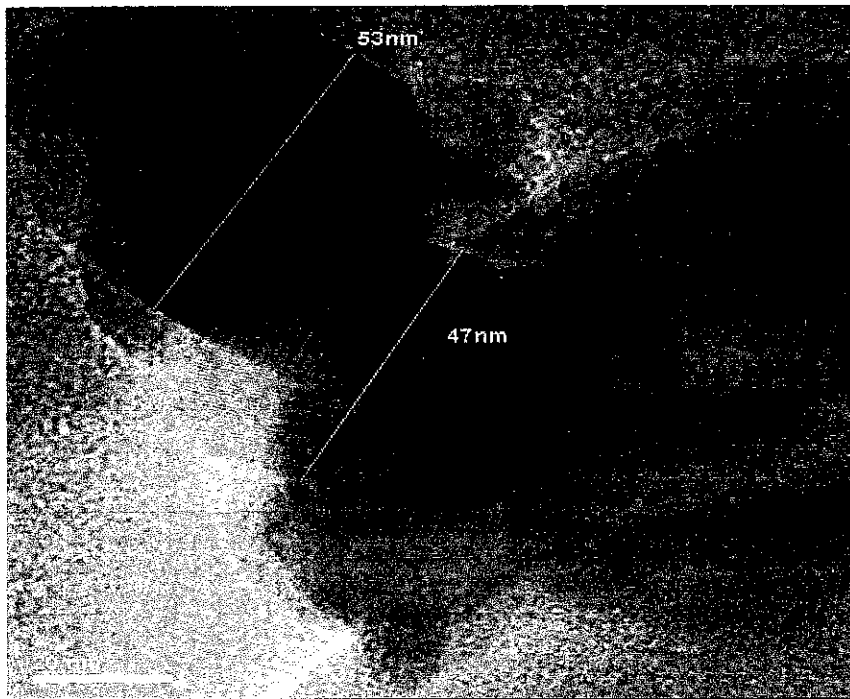


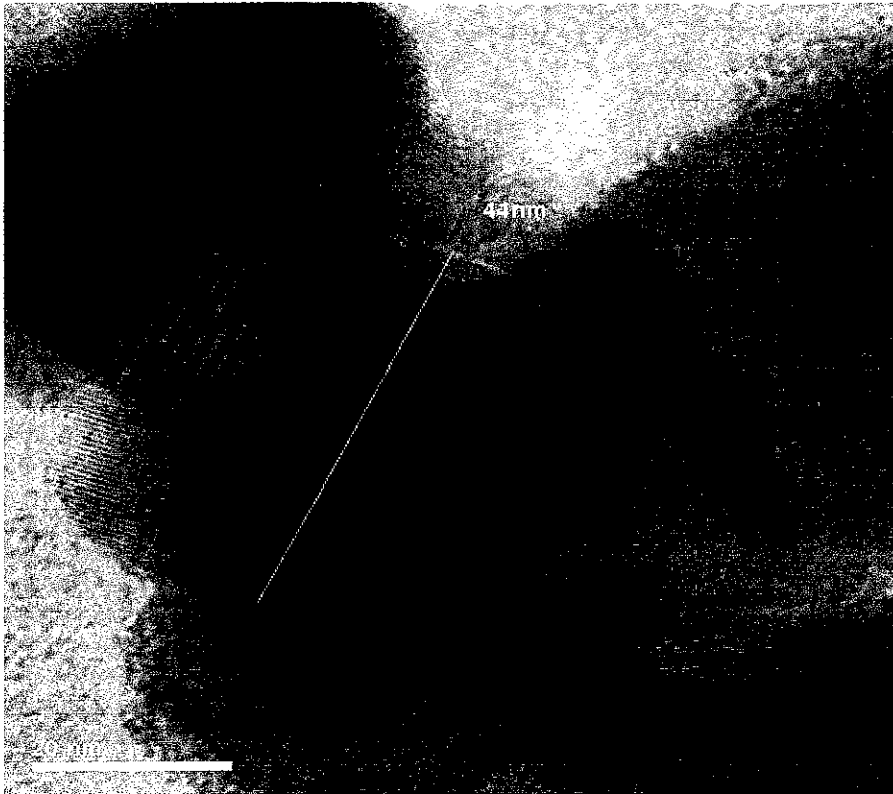
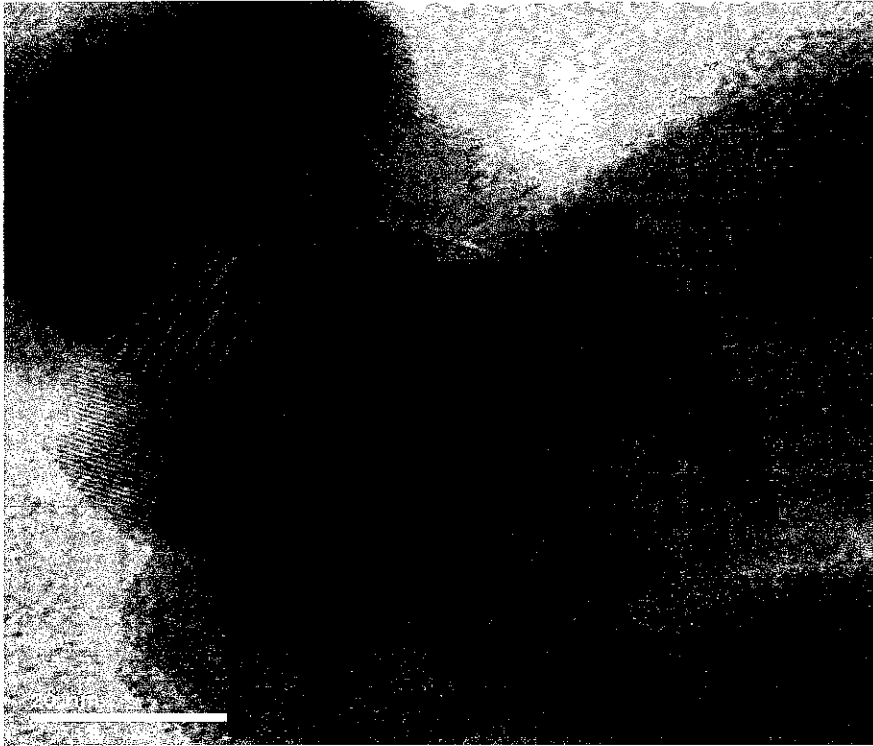


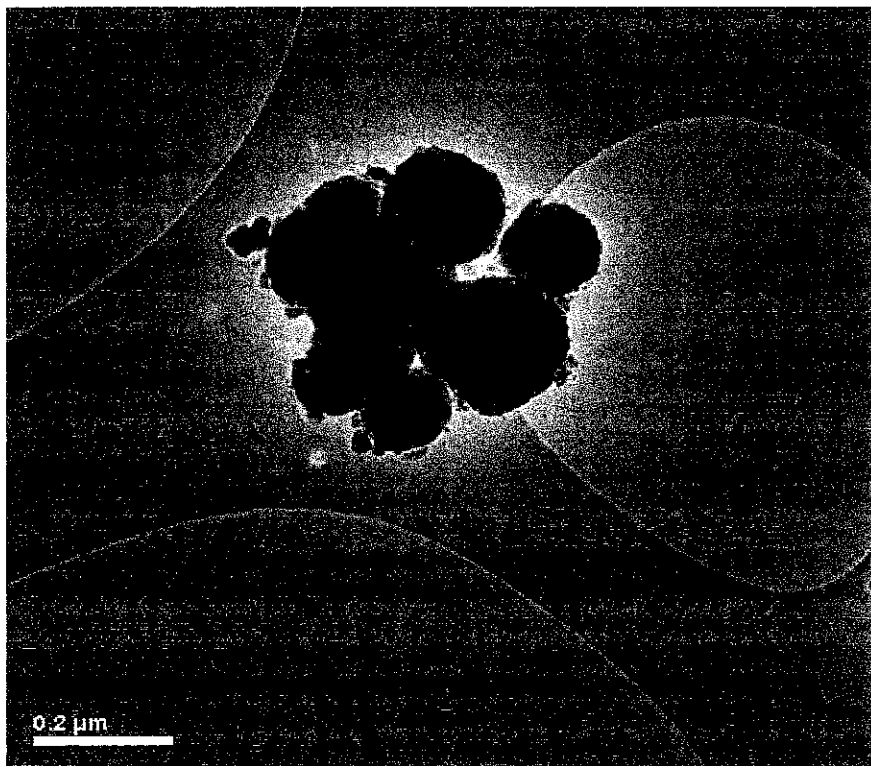
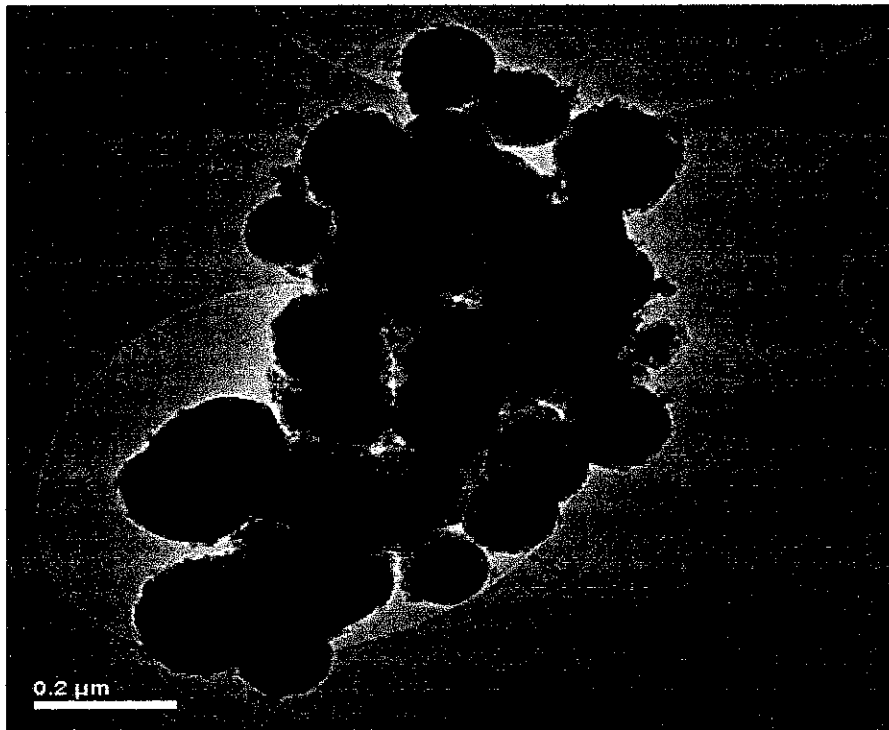


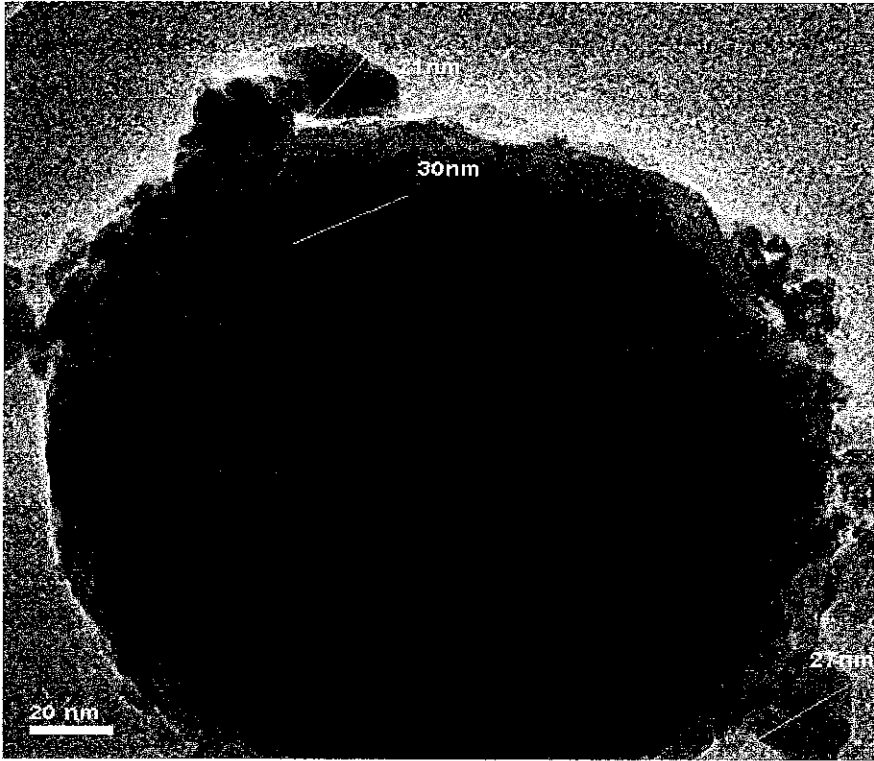




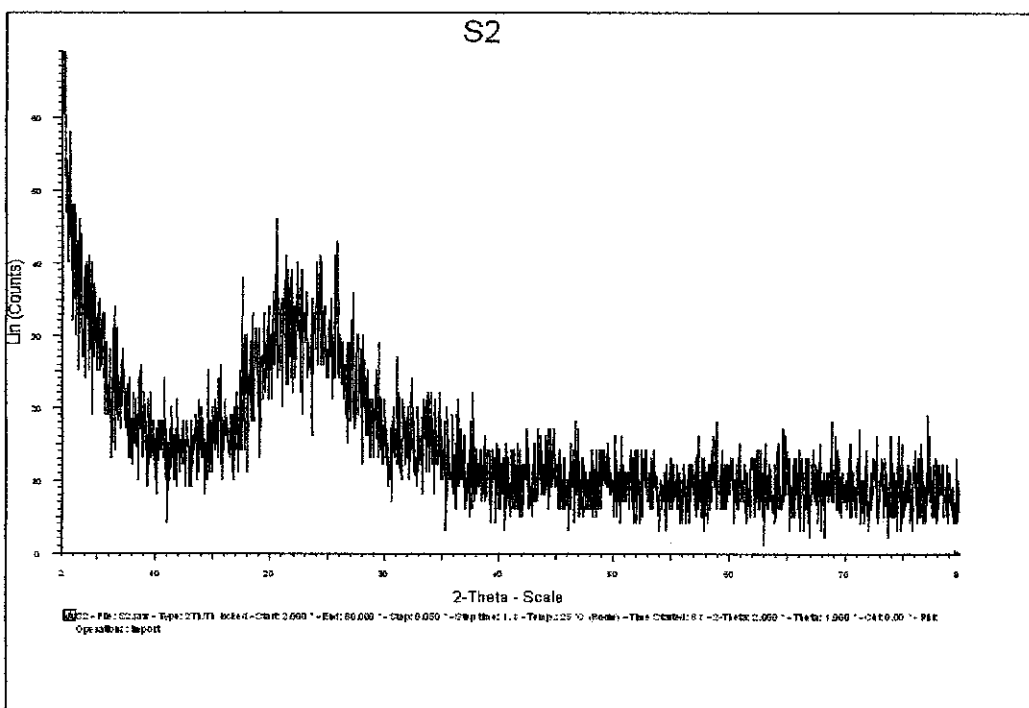
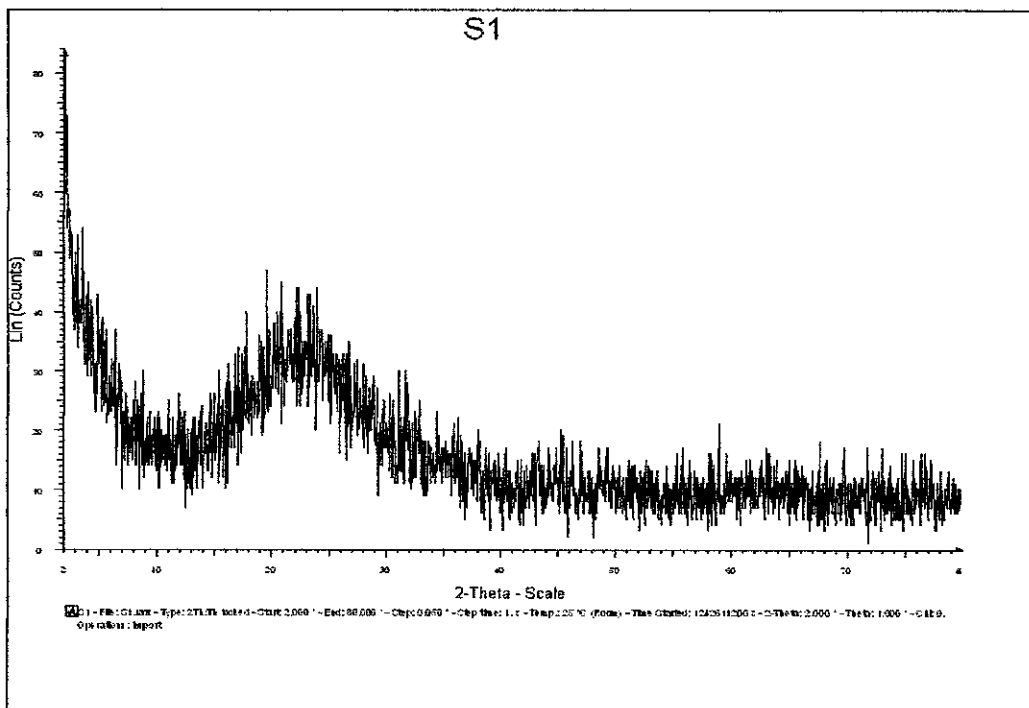




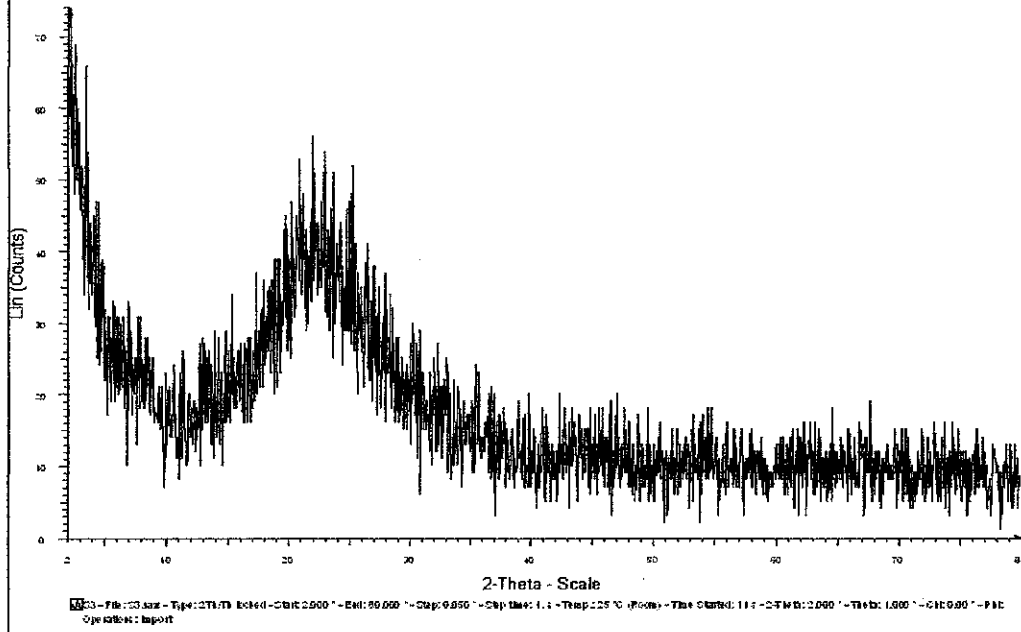




APPENDIX E: X-RAY DIFFRACTION (XRD) IMAGES OF Fe/SiO₂ CATALYST



S3



S4

